nature communications

Article

https://doi.org/10.1038/s41467-024-53845-7

A molecular toolkit for heterologous protein secretion across *Bacteroides* species

Received: 24 December 2023

Accepted: 23 October 2024

Published online: 11 November 2024

Check for updates

Yu-Hsuan Yeh[1,2], Vince W. Kelly[1,7], Rahman Rahman Pour[1,8] & Shannon J. Sirk[1,2,3,4,5,6]

Bacteroides species are abundant, prevalent, and stable members of the human gut microbiota, making them a promising chassis for developing long-term interventions for chronic diseases. Engineering *Bacteroides* as in situ bio-factories, however, requires efficient protein secretion tools, which are currently lacking. Here, we systematically investigate methods to enable heterologous protein secretion in *Bacteroides*. We identify a collection of secretion carriers that can export functional proteins across multiple *Bacteroides* species at high titers. To understand the mechanistic drivers of *Bacteroides* secretion, we characterize signal peptide sequence features, post-secretion extracellular fate, and the size limit of protein cargo. To increase titers and enable flexible control of protein secretion, we develop a strong, self-contained, inducible expression circuit. Finally, we validate the functionality of our secretion carriers in vivo in a mouse model. This toolkit promises to enable expanded development of long-term living therapeutic interventions for chronic gastrointestinal disease.

Engineered living therapeutics comprise an emerging class of microbial cell-based treatment strategies utilizing both native and modified strains to function as biological machines that mediate disease prevention and treatment from within the human body. Achievements in this field are driven by a continuous expansion of our knowledge of host-microbiota interactions[1] combined with ongoing innovations in synthetic biology tools[2]. These advances have supported numerous studies demonstrating that commensal gut bacterial species can be engineered to perform metabolic functions[3–6] or produce and deliver therapeutic compounds from within the gastrointestinal (GI) tract[4,7–11]. Notably, ~90% of the bacterial species in the average human gut belong to only two phyla – *Bacteroidetes* and *Firmicutes*[12]– and ~25% of the entire microbial community in the colon belongs to a single dominant genus: *Bacteroides*[13]. Furthermore, a longitudinal study of human gut microbiota stability of healthy adults in the United States showed that the colonization of *Bacteroides* species can remain stable for up to five years[14]. Together, these features potentiate the use of *Bacteroides* species as a robust chassis for developing living therapeutics to achieve in situ, long-term treatment and monitoring of chronic diseases such as cancer, diabetes, and inflammatory bowel diseases (IBD). Critically, recent extensive studies of *Bacteroides* species provide a powerful selection of tools for genetic manipulation[15–23], biocontainment[24], and tunable engraftment[25], further advancing their application from bench to bedside.

When engineering bacteria for therapeutic or diagnostic purposes in which protein-based products must function in the extracellular space, the ability of the microbial chassis to secrete heterologous cargo is a key selection criterion[26,27]. While the *Bacteroides* genus represents an attractive collection of target species for this purpose, all *Bacteroides* species are Gram-negative, which presents technical challenges for efficient protein secretion. Unlike Gram-positive bacteria, which have a single lipid membrane and readily secrete heterologous

[1]Department of Bioengineering, University of Illinois Urbana-Champaign, Urbana, IL, USA. [2]Chan Zuckerberg Biohub, Chicago, IL, USA. [3]Department of Biomedical and Translational Sciences, Carle Illinois College of Medicine, Urbana, IL, USA. [4]Department of Microbiology, University of Illinois Urbana-Champaign, Urbana, IL, USA. [5]Carl R. Woese Institute for Genomic Biology, University of Illinois Urbana-Champaign, Urbana, IL, USA. [6]Cancer Center at Illinois, University of Illinois Urbana-Champaign, Urbana, IL, USA. [7]Present address: Department of Chemical and Biological Engineering, University of Colorado Boulder, Boulder, CO, USA. [8]Present address: Perlumi, Berkeley, CA, USA. e-mail: sirk@illinois.edu

cargo outside of the cell through both the general secretion pathway (Sec) and the twin-arginine translocation (Tat) pathway as long as the target protein is fused to an appropriate signal peptide (SP)[28,29], protein secretion from double-membraned Gram-negative bacteria is more complex and requires additional cellular machinery[30]. Thus far, eleven different secretion systems have been identified in Gram-negative bacteria, referred to as the type 1 secretion system (T1SS) through T11SS[30,31]. Some of these secretion systems are well characterized and widely used for heterologous protein secretion in non-native hosts, such as T1SS[32] and T3SS[33–35]. However, these secretion systems are either poorly conserved or completely absent from all *Bacteroides* species studied to date[36,37]. A few studies have reported that fusing a therapeutic protein with SPs from *Bacteroides fragilis* enterotoxin (BFT) or OmpA (BT_3852) of *Bacteroides thetaiotaomicron* (*B. theta*)[15,38–40] yields detectable levels of secretion; however, the highest reported titer of ~10 ng/mL[40] is still orders of magnitude lower than the secretion titers observed with other well-studied Gram-negative and Gram-positive bacteria, often exceeding 100 μg/mL[28,41].

Here, to address these limitations and capitalize on the potential of *Bacteroides* species as a powerful platform for developing engineered living therapeutics, we systematically investigate the heterologous protein secretion capability of both endogenous and exogenous secretion systems in *B. theta*, a highly studied species that is representative of the genus within the human gut microbiota. Our investigations reveal a suite of full-length proteins and lipoprotein SPs derived from native *B. theta* secretory proteins that can deliver functional antibody fragments and reporter proteins into the extracellular space. We show that these secretion carriers are broadly functional across multiple *Bacteroides* species. We also define the sequence features and preferred amino acid composition of lipoprotein SPs that can drive high-level secretion. To further refine the usage of secretion carriers, we evaluate the post-secretion fate of protein cargo exported via full-length fusion partners and lipoprotein SPs and observe both outer membrane vesicle (OMV)-dependent and OMV-independent secretion. By selecting specific secretion carriers from our collection, we are able to direct secreted proteins to specific target destinations: freely soluble in the extracellular space; bound to the external surface of OMVs; or held within the OMV lumen. Additionally, toward full characterization and optimization of our system, we identify a putative cargo size limit for lipoprotein SP-mediated secretion of heterologous proteins and also develop a strong, self-contained, inducible system for driving robust protein expression in *Bacteroides* species. Finally, we verify the in vivo activity of our platform using *B. theta* engineered for in situ delivery of the bioluminescent reporter NanoLuc, which we quantify ex vivo in fecal homogenates. The molecular toolkit provides an accessible framework for generating living therapeutic and diagnostic machines from highly relevant human commensal *Bacteroides* species.

Results

P_{BfP1E6}-RBS8 drives strong and reproducible secretion of proteins in *B. theta*

To establish a set of secretion tools for members of the *Bacteroides* genus, we selected *B. theta* as the starting point based on its prevalence and abundance in the human gut as well as the large body of knowledge surrounding this species, including a substantial collection of well characterized genetic tools[15–23]. To ensure robust and reproducible results, we first sought to establish a framework for evaluation of protein expression and secretion across diverse samples. We identified a core set of three native *B. theta* proteins previously shown to be highly secreted, each with a different N-terminal signal sequence: BT_2472 (Sec/SPI SP), BT_3382 (lipoprotein SP), and BT_3769 (no SP identified; secretion mechanism unknown)[42]. To identify optimal genetic parts for reproducible and detectable protein secretion, we tested each protein using three different promoter/ribosome-binding site (RBS) pairs (Fig. 1a). For strong, constitutive expression, we used a previously characterized *Bacteroides fragilis* phage promoter paired with either its original RBS (RBS_{phage}) or a modified version with the highest observed activity amongst reported variants (RBS8)[19]. For more precisely controlled protein expression, we used a tightly regulated anhydrotetracycline (aTc)-inducible promoter ($P1T_{DP}$-GH023)[17]. To evaluate the performance of the different constructs and to determine the best timepoint for measuring extracellular protein accumulation in future studies, we expressed each protein from each expression plasmid and monitored bacterial growth and secretion in *B. theta* liquid culture for 48 h (Fig. 1b). Despite similar growth kinetics between samples, we only observed high levels of secretion from BT_3382, and only with the strong, constitutive phage promoter/RBS pairs. BT_3769 only achieved levels of secretion above background when expression was driven by P_{BfP1E6}-RBS8, however the signal was more than two-fold lower than that measured for BT_3382 with the same promoter/RBS. Interestingly, $P1T_{DP}$-GH023 did not drive high enough protein expression to result in detectable levels of secretion for any of the three proteins, even after doubling the concentration of aTc from 100 ng/mL to 200 ng/mL (Fig. 1b). Similarly, no expression construct produced detectable levels of secreted BT_2472 (Fig. 1b). It is possible that the C-terminal domain of this protein is involved in secretion and was compromised by the 3xFLAG tag that was included for immunodetection.

For both BT_3382 and BT_3769, we observed peak extracellular protein accumulation when *B. theta* cultures grew to late log phase (16–20 hr, OD_{600} 0.6–0.8). Beyond this point however, the amount of BT_3769 in the culture media rapidly dropped to undetectable levels within 8 h, whereas the level of BT_3382 only dropped by ~15% when measured 48 hr later (Fig. 1b). The persistently high levels of BT_3382 may be due to higher protein stability rather than continued production and secretion by *B. theta* during stationary growth as BT_3382 is reported to be enriched in OMVs[42], which may lead to higher thermostability[43,44].

Based on these results, we decided to 1) use P_{BfP1E6}-RBS8 as our baseline promoter/RBS pair to drive expression of all constructs moving forward since it resulted in the highest observed secretion levels in this preliminary screen, and 2) collect all supernatant samples between late log and stationary phase of growth to ensure consistent detection of secreted products within the predicted window of protein stability for all samples.

Identification of *B. theta* secretion carrier candidates from endogenous and exogenous sources

To continue developing our secretion toolkit, we next sought to identify signal peptides, full-length proteins, or protein domains that function as secretion carriers that promote extracellular export of heterologous proteins from *B. theta*. Similar approaches either utilize endogenous secretion machinery with homology to known systems or introduce exogenous secretion systems/tags from other bacterial strains[41]. Because most previously characterized secretion systems in Gram-negative bacteria are either incomplete or not conserved in the *B. theta* genome[36,37], the endogenous secretion systems of *B. theta* are still poorly understood. To circumvent this limitation, we identified three secretion strategies that are typically applicable to all Gram-negative bacteria—leaky outer membrane (OM), fusion partner, and outer membrane vesicle (OMV) (Fig. 1c) – and searched for endogenous secretion carrier candidates within each of these categories in *B. theta* genome. The leaky OM strategy relies on transport of proteins into the periplasm via the Sec pathway, followed by secretion to the extracellular space through natural OM leakage[41] (Fig. 1c). We selected two Sec/SPI SPs from two *B. theta* endogenous proteins as candidate secretion carriers for the leaky OM strategy: SusB, a periplasmic protein of the well-studied *B. theta* starch utilization system (Sus)[45], and BT_3769, which was previously identified as highly secreted[42]. The

https://doi.org/10.1038/s41467-024-53845-7

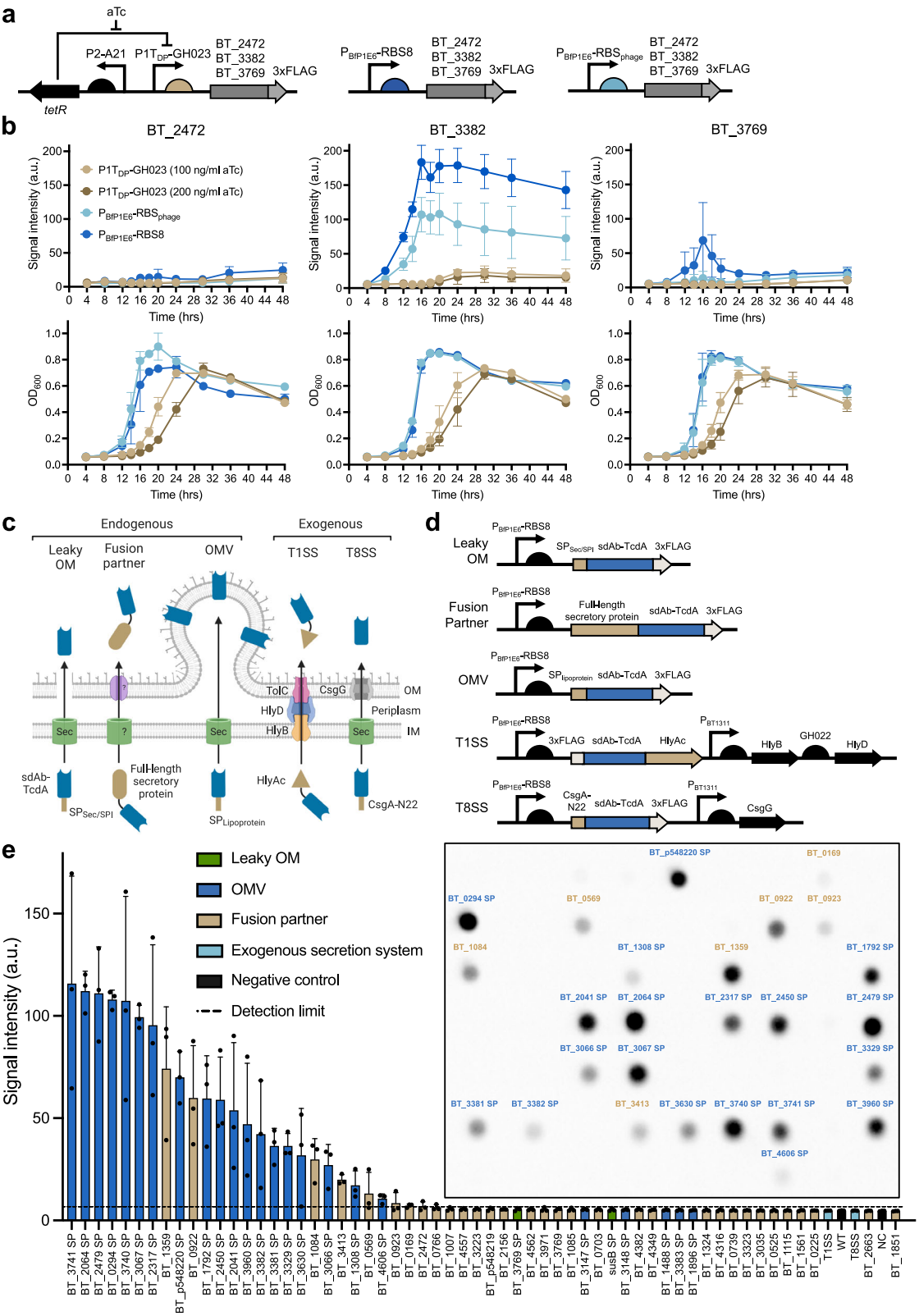

fusion partner strategy employs genetic fusion of heterologous cargoes with full-length native secretory proteins for co-transportation out of the cell[41] (Fig. 1c), without the need to understand the underlying secretion mechanisms. To search for secretion carriers for the fusion partner strategy, we referred to a previous study characterizing endogenous protein abundance in different fractions (inner membrane [IM], OM, OMV pellets [OMVp], and OMV-free supernatants [SUP]) of *B. theta* liquid culture[42] and identified thirty-three candidates with high abundance in the OMVp, SUP, or both fractions (Supplementary Data 1 and 2, Methods). Finally, the OMV strategy is based on the recent discovery of the lipoprotein export signal (LES), a five-residue conserved motif that immediately follows the lipoprotein SP cleavage site (+2 to +6) in many native OMV-enriched lipoproteins in *B. theta*[42,46]. We hypothesized that adding a lipoprotein SP with an

Fig. 1 | Engineering *B. theta* to secrete sdAb-TcdA. a Design of genetic constructs for protein expression and secretion. **b** Protein secretion (top row) and growth (bottom row) of *B. theta* expressing 3xFLAG-tagged BT_2472, BT_3382, or BT_3769 with their native secretion signals, measured from supernatant samples collected over 48 hrs. Protein levels were measured by dot blot and bacterial growth was measured by optical density at 600 nm (OD_{600}). For strains using the $P1T_{DP}$-GH023 promoter, the inducer aTc (100 or 200 ng/mL) was included in the medium at the time of inoculation. Data are presented as the mean ± standard deviation of three biological samples. a.u., arbitrary units. **c** Schematic representation of secretion strategies explored in this study. **d** Design of genetic constructs for secretion carrier screening in *B. theta*. **e** Relative levels of secretion of sdAb-TcdA in culture supernatants of *B. theta* harboring sixty different expression/secretion constructs, measured by dot blot. Inset shows representative dot blot with effective secretion carriers (above detection limit) labeled. Detection limit (dotted line) was set at the signal intensity of the faintest dot visible by unaided eye on the membrane, ~7 a.u. Data are presented as the mean ± standard deviation of three biological samples. WT, wild-type *B. theta*; NC, negative control *B. theta* expressing sdAb-TcdA with no secretion carrier fusion. Panel (**c**) Created in BioRender. Yeh, Y. (2022) BioRender.com/v42q089. Source data are provided as a Source Data file.

identifiable LES to heterologous cargoes would enable their secretion via OMVs (Fig. 1c). Using the same data set as for the fusion partner strategy, we identified the SPs of twenty-four lipoproteins enriched in either the OMVp or the combined (OMVp+SUP) fractions of *B. theta* liquid culture as candidate secretion carriers for the OMV strategy[42] (Supplementary Data 1 and 2, Methods).

We also selected two highly studied secretion systems from *Escherichia coli*–T1SS and T8SS (Fig. 1c)—based on their small genetic size, few components, and simple regulation to ensure the highest chance of success. The hemolysin system (T1SS) of uropathogenic *E. coli* (UPEC)[47] and the curli system (T8SS) from *E. coli* K-12[48], have both been used successfully for heterologous protein secretion in non-native hosts[49,50]. The hemolysin system contains HlyB, HlyD, and TolC, which form the secretion channel, and HlyA, which is the cognate secreted product used to drive co-transport of protein cargoes via fusion to its C-terminal domain (HlyAc) (Fig. 1c, Supplementary Data 2). We fused the HlyAc domain to the C-terminus of the secreted protein cargo and inserted the HlyB and HlyD genes into the same plasmid in a polycistronic format under the control of the strong native *B. theta* constitutive promoter P_{BT1311} with the *B. theta* GH022 RBS[18] (Fig. 1d). We did not include TolC in this construct because it is conserved in most bacterial species[51] and several putative homologs exist in *B. theta*[52]. The curli secretion system (T8SS) is even simpler than the hemolysin system, requiring only a CsgG transport protein (expressed by P_{BT1311}) and an N-terminal fusion of the first 22 amino acids of the cognate secreted product (CsgA-N22) to the cargo protein[50] (Figs. 1c, d, Supplementary Data 2).

To evaluate the efficiency of the sixty-one secretion carriers described above, we selected a single candidate protein to serve as our standard secretion cargo. Because our goal is to establish a toolbox to enable the development and implementation of *Bacteroides* species as living therapeutics in their natural gut environment, we selected a clinically relevant single domain antibody (sdAb) that targets Toxin A (TcdA) from *Clostridioides difficile*[53], a prominent and challenging gastrointestinal pathogen[54]. Compared to full-length antibodies, the small size and structural simplicity of sdAbs allows them to be more easily expressed by bacteria and results in higher thermal and proteolytic stability in the harsh gut environment. Except for HlyAc, all candidate secretion carriers (candidate SP or full-length carrier protein) were fused to the N-terminus of sdAb-TcdA with a C-terminal 3xFLAG tag for detection (Fig. 1d).

Native *B. theta* secretion carriers enable high-level extracellular export of sdAb-TcdA

Of the sixty-one secretion carriers we identified (Supplementary Data 2) and fused to sdAb-TcdA, all constructs were successfully cloned and conjugated into *B. theta* except for BT_3434, which appeared to be lethal in *E. coli* DH5α. To determine the secretion efficiency of each of the other sixty secretion carriers, we grew *B. theta* transconjugant cultures to late-log phase and measured the abundance of sdAb-TcdA in culture supernatant by dot blot (Fig. 1e). Twenty-six (43%) of the secretion carriers produced visible signal and were thus considered effective. No candidate from the leaky OM nor the exogenous secretion system approaches were represented in this group, which may be due to the need for membrane-disrupting methods for full efficacy with the leaky OM approach[55,56], and the need for unknown accessory proteins or regulators that are not conserved in *B. theta* with *E. coli* T1SS and T8SS[48,57,58]. Of the twenty-six effective secretion carriers, seven (27% of effective candidates, 12% of total) are full-length fusion partner proteins (six with Sec/SPI SPs and one with a lipoprotein SP) and nineteen (73% of effective candidates, 32% of total) are lipoprotein SPs. The seven effective fusion partners represent only 22% of the thirty-two total fusion partners tested. The relatively low success rate of this class of secretion carrier could be improved with optimization of the fusion, e.g., truncation mutants, alternate orientations (N-, C-, or in-frame internal fusions), etc.[59–61]. Conversely, the efficient secretion of sdAb-TcdA observed for 79% of the lipoprotein SPs (19/24) supports our hypothesis that lipoprotein SPs with LES sequences may be able to drive OMV-mediated secretion of heterologous proteins.

A positively charged region and length-restricted hydrophobic region are critical for effective heterologous protein secretion by lipoprotein SPs

Most of the effective secretion carriers we identified were lipoprotein SPs from the OMV secretion strategy, however, five *B. theta* lipoprotein SPs that we tested did not effectively mediate secretion of sdAb-TcdA: BT_1488, BT_1896, BT_3147, BT_3148, and BT_3383 (Fig. 1e). To determine if effective lipoprotein SPs harbor other unique features in addition to the LES, we analyzed their amino acid sequences. Lipoprotein SPs are composed of a positively charged N-terminal region (n), a central hydrophobic region (h), a cysteine residue after the cleavage site (+ 1), and a LES motif (+ 2 to +6). Interestingly, we found that the backbones (n- and h- regions) of the five ineffective lipoprotein SPs are either very short (~10 residues) or very long (~40 residues), compared to the backbones of effective lipoprotein SPs (16-34 residues) (Fig. 2a). All five ineffective lipoprotein SPs lack a positively charged n-region and BT_3383 SP also has no clear h-region (Fig. 2b). These results suggest that, in addition to the LES, the presence of positively charged residues in the n-region, as well as a minimum length of the h-region may be critical factors that drive lipoprotein SP-mediated secretion in *B. theta*.

To test this hypothesis, we swapped the n- and h-regions of the five ineffective SPs with those from an effective SP to see if we could improve their secretion efficiency through rational design. We chose the SP from BT_3630 as our standard based on its layout of charged and hydrophobic regions, which is broadly representative of the collection of lipoprotein SPs that we identified as effective (Fig. 2b, c). For each of the five ineffective lipoprotein SP sequences, we made the following three SP variants and fused them to the sdAb-TcdA: 1) added two N-terminal lysines immediately after the start codon to introduce the positively charged region (SP-N), 2) replaced the hydrophobic region with the one from BT_3630 SP (SP-H), or 3) introduced both modifications (SP-NH) (Fig. 2c). The only variant that was not generated was the SP-N version of the BT_3383 SP; because it does not have an obvious h-region we concluded that

https://doi.org/10.1038/s41467-024-53845-7

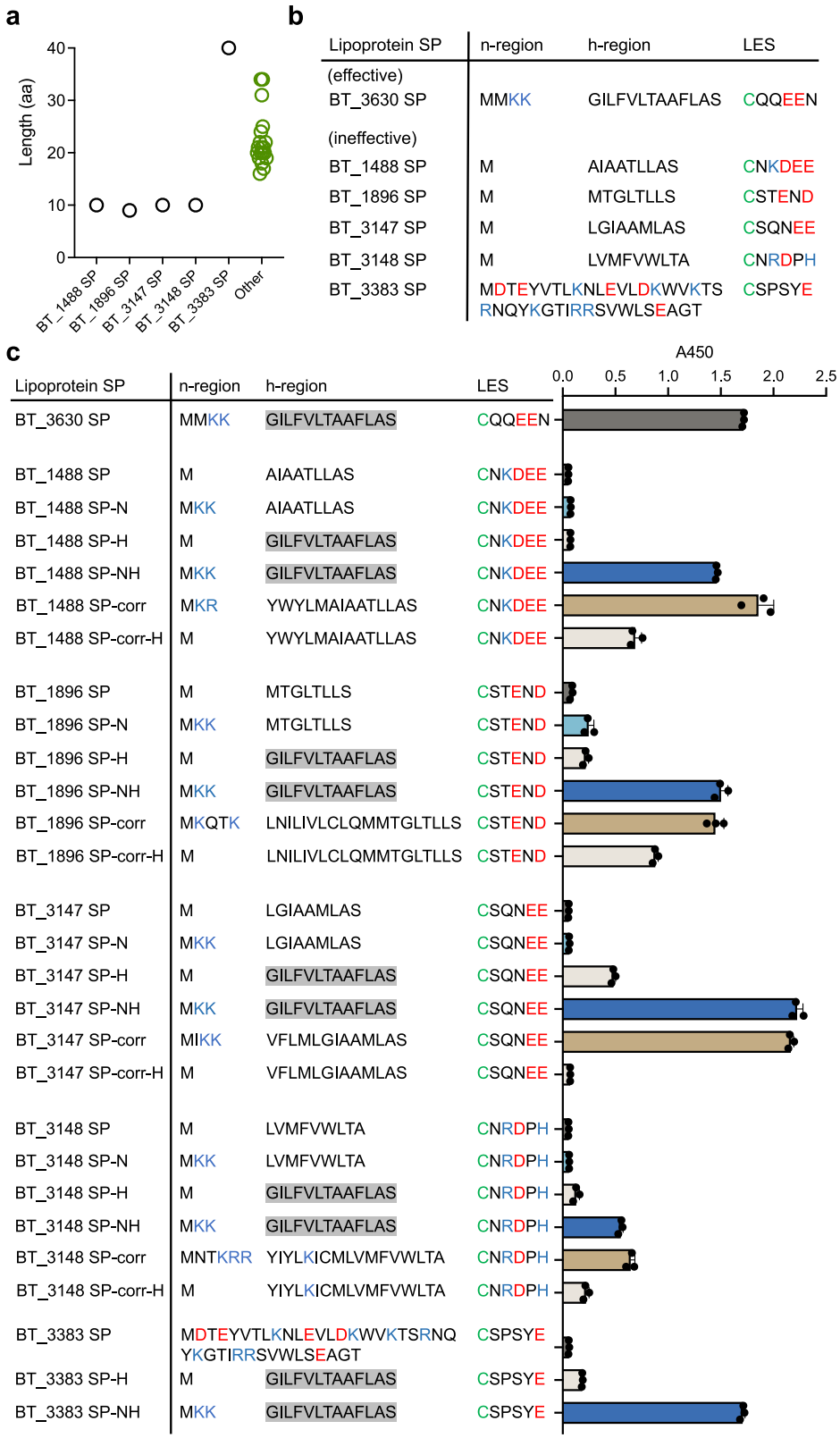

Fig. 2 | Rational engineering enables ineffective lipoprotein SPs to secrete sdAb-TcdA. a Comparison of the length of five ineffective (black) and nineteen effective (green) lipoprotein SPs. **b** Comparison of amino acid sequences of the five ineffective lipoprotein SPs with the sequence of effective BT_3630 SP. Residue coloring: blue, positive charge; red, negative charge; cysteine, green. **c** Secretion of sdAb-TcdA driven by the SP variants of BT_1488, BT_1896, BT_3147, BT_3148, and BT_3383, measured by ELISA. BT_3630 SP-sdAb-TcdA is included as a positive control. Residue coloring is as for (**b**), the hydrophobic regions of BT_3630 SP are boxed in gray. Data are presented as the mean ± standard deviation of three biological samples. Source data are provided as a Source Data file.

addition of an n-region would not be sufficient to improve its secretion capability.

We observed enhanced secretion of the sdAb-TcdA only for SPs that had both an added N-terminal charged domain and a swapped hydrophobic region (SP-NH variants) (Fig. 2c), suggesting that both regions are necessary, but neither is sufficient to drive high-level secretion in *B. theta*. Notably, the increase in sdAb secretion measured for the BT_3148 SP-NH variant was substantially lower than for the other SP-NH variants (Fig. 2c). Inspection of the LES sequence revealed positively charged amino acids at the +3 and +6 positions, which is consistent with previous findings showing that positively charged amino acids can offset LES-mediated OMV secretion[42]. Notably, close inspection of the *B. theta* genome revealed alternative start codons for BT_1488, BT_1896, BT_3147, and BT_3148, which result in incorporation of a positively charged n-region and extended h-region for all four SPs (Supplementary Fig. 1). We generated these four corrected SPs (suffixed -corr) and variants with only the h-region (suffixed -corr-H) and measured sdAb-TcdA secretion efficiency for each (Fig. 2c). Consistent with the results of previous SP engineering, the four corrected SPs mediated significant sdAb-TcdA secretion compared to the original SPs, which was disrupted upon exclusion of the charged n-regions (Fig. 2c). These results begin to define the requirements for the presence and placement of charged and hydrophobic residues in highly effective *B. theta* lipoprotein SP sequences.

B. theta secretion carriers mediate export of multiple types of functional protein cargoes

Toward our goal of establishing a flexible toolbox to enable efficient secretion of diverse heterologous protein cargoes, we next tested the ability of the twenty-six effective secretion carriers (Fig. 1e) to secrete six additional proteins with therapeutic and/or diagnostic functions. Three of the six proteins are disease-targeting antibody fragments, including an sdAb targeting tumor necrosis factor alpha (sdAb-TNFα)[62], an antigen associated with chronic conditions such as inflammatory bowel disease (IBD)[63]; another sdAb targeting epidermal growth factor receptor (sdAb-EGFR)[64], commonly overexpressed in colon cancer[65]; and a single-chain variable fragment targeting human epidermal growth factor receptor-2 (scFv-HER2)[66], mainly known for its role in breast cancer, but also implicated in colon cancer[67]. This set of proteins allows us to evaluate secretion efficiency across diverse antibody fragment formats while still focusing on targets relevant to gastrointestinal delivery by engineered living therapeutics. We selected the other three proteins to provide a diverse set of reporter functions: NanoLuc (Nluc)[68], enhanced green fluorescent protein (EGFP)[69], and β-lactamase (BLac)[70], which yield quantifiable outputs of luminescence, fluorescence, or colorimetric signal, respectively.

Each of these six cargo proteins were fused to each of the twenty-six secretion carriers, resulting in one hundred and fifty-six new carrier-cargo pairs. With the exception of EGFP, all cargoes were secreted from *B. theta* and accumulated at varying levels in culture supernatants via different secretion carriers (Fig. 3a). The exceptionally low levels of EGFP detected in culture media may be due to rapid folding of this protein, which has been reported to stall the translocon complex during the secretion process[71]. For the other cargoes, we observed considerable variability in secretion efficiency both between different secretion carriers and amongst cargoes secreted by the same carrier. In contrast to EGFP, we detected secreted Nluc at high levels across the majority of secretion carriers, suggesting that Nluc can be broadly used as a highly sensitive reporter for measuring secretion efficiency. Compared to the other proteins tested, Nluc has a higher solubility and a more acidic isoelectric point (Supplementary Table 1), both of which have been reported to enhance protein secretion[72,73].

To verify that the secreted protein products were properly folded and not otherwise functionally disrupted by fusion to the secretion carriers, we performed functional assays to measure the antigen binding or enzymatic activity of each of the secreted cargo proteins in *B. theta* culture supernatants. Because the readouts of these functional assays are not equivalent across cargoes (Supplementary Fig. 2), we scaled the output values to a normalized range of zero to one, corresponding to the lowest and highest readout for each cargo across the twenty-six secretion carriers (Fig. 3b, lower panel). We then created a functional secretion score for each carrier by summing the normalized functional outputs for all six cargo proteins for each secretion carrier (Fig. 3b, upper panel). These results revealed several lipoprotein SPs that are broadly effective for secreting diverse cargoes with BT_3630 SP and BT_3067 SP emerging as the most consistent and robust broadly active secretion carriers. To further verify that secreted antibody fragments retain their native function, we measured the TNF neutralizing activity of bacterially secreted sdAb-TNFα on murine L929 cells[74] and observed a correlation between TNF-neutralizing activity and bacterial secretion efficiency; the highest efficiency sdAb-TNFα secretion carriers mediated the highest levels of neutralizing activity, comparable to the saturated signals observed with 10 and 50 μg/mL of purified sdAb-TNFα (Fig. 3c). These results also indicate that fusion to secretion carriers does not disrupt the therapeutically relevant function of the sdAb cargo. Finally, to quantify the efficiency of our approach compared to previously reported *Bacteroides* secretion tools, we generated Nluc constructs fused to BT_3852 (OmpA) SP[40] or *B. fragilis* enterotoxin (BFT) SP[15,38,39] and measured their secretion efficiency in *B. theta*. Compared to a set of three secretion carriers representing a range of secretion efficiency identified in this study, our constructs demonstrated ~4- to 17-fold and 950- to 4000-fold higher luminescence than OmpA or BFT SP respectively (Supplementary Fig. 3).

Interestingly, although all sdAbs share a similar structure[75], the three sdAbs tested here were not secreted at similar levels by the same secretion carriers. It has been reported that cargo-specific interactions with signal peptides can indirectly impact secretion by influencing other cellular processes such as protein biosynthesis, folding kinetics, and structural stability[76], which could explain some of this variability. Indeed, we further quantified the concentration of the above secretion carrier-fused antibody fragments and Nluc from equivalent volumes of cell pellets and supernatants of *B. theta* liquid culture, revealing that the overall protein levels (cell pellet + supernatant) varied across different secretion carriers and seemed positively correlated with their secretion efficiency (Supplementary Fig. 4). These data suggest that highly efficient secretion carriers may support high level protein expression by unknown mechanisms. It is also possible that low efficiency secretion carriers prevent protein export to such an extent that they cause protein aggregation and the formation of inclusion bodies, which would not be detected in our assay and would artificially decrease the protein abundance detected in those cell pellets.

B. theta-derived secretion carriers function across multiple *Bacteroides* species

Toward the goal of developing universal secretion tools for the *Bacteroides* genus, we next evaluated the *B. theta*-derived secretion carriers in other *Bacteroides* species. We selected the ten carriers with the highest functional secretion scores (Fig. 3b) and measured secretion (Fig. 4a) and functionality (Fig. 4b) of each of the six cargo proteins when expressed in three different *Bacteroides* species: *B. fragilis, B. ovatus*, and *B. vulgatus*. We were unable to generate *B. fragilis* transconjugants for six of the carrier-cargo pairs, which may be due to low conjugation efficiency in this species[19] or lethal intracellular aggregation of protein cargoes[77]. For all other *Bacteroides* transconjugants, the results mirrored those observed in *B. theta* (Fig. 3); secretion efficiency varies not only between cargoes but also between species. Among the *Bacteroides* species tested, *B. ovatus* generally demonstrated the highest secretion activity for any given carrier-cargo pair, which may be due to the closer phylogenetic relationship between *B. theta* and *B.*

https://doi.org/10.1038/s41467-024-53845-7

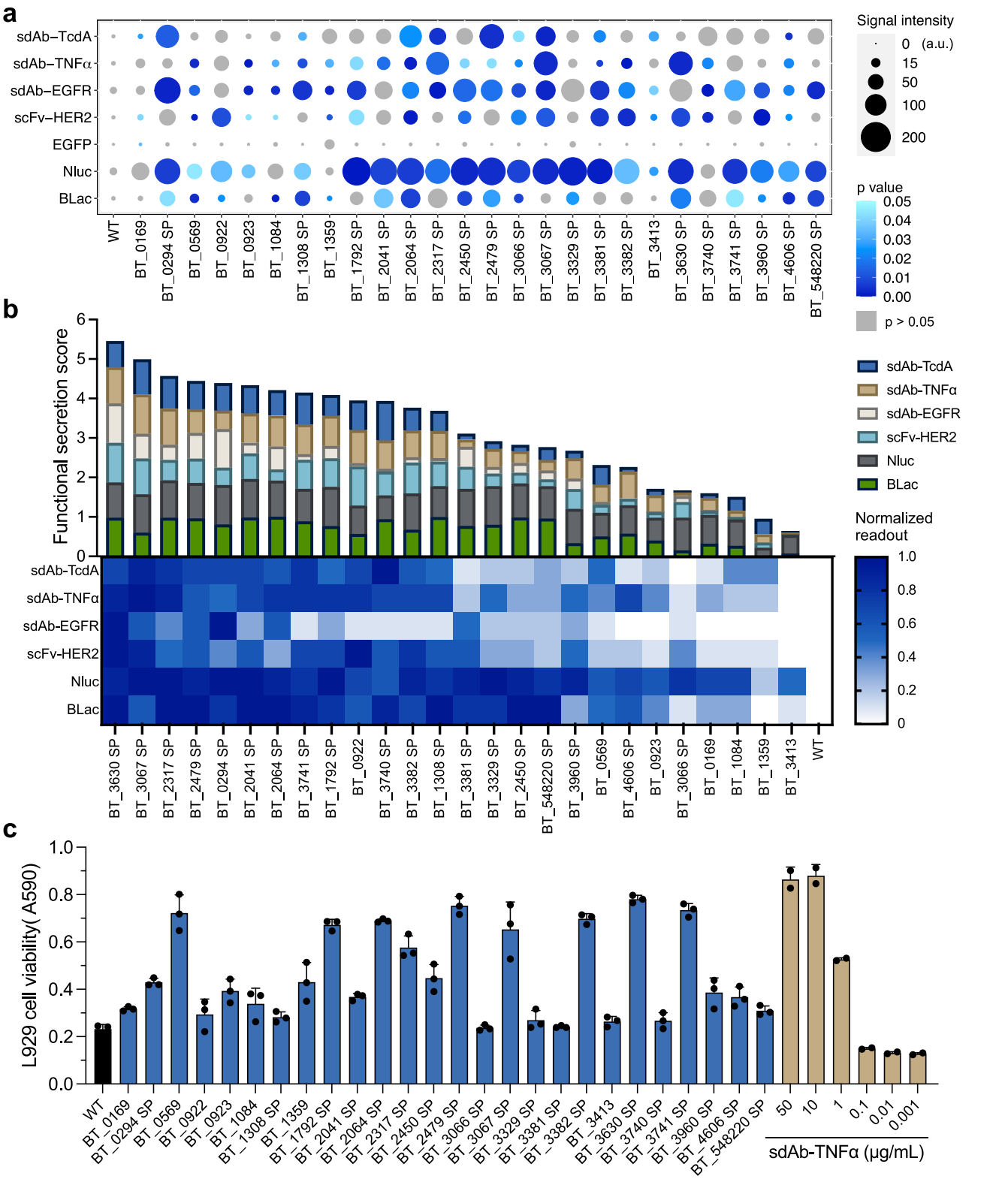

Fig. 3 | *B. theta*-derived secretion carriers function across multiple heterologous proteins. a Relative levels of antibody fragments and reporter proteins secreted into culture supernatant by *B. theta* secretion carriers. Bubble size corresponds to average dot blot signal intensity of three biological samples with $p < 0.05$ indicated by the blue color scale and $p > 0.05$ shown in gray. Significance was determined using unpaired two-tailed Welch's *t* test. (**b**) Functional assays of antibody fragments and reporter proteins secreted into culture supernatant by *B. theta* secretion carriers. Binding of antibody fragments (sdAbs and scFv) to their respective targets was determined by ELISA. Enzymatic activity of reporter proteins Nluc and BLac was determined by bioluminescence assay and colorimetric assay, respectively. Following log transformation of luminescence data, all functional assay readouts were converted to values between zero and one by cargo-wise min-max normalization. Functional secretion scores were calculated by summing the average normalized readouts of all cargoes for each secretion carrier. **c** Viability of L929 cells after treating with pre-incubated mixture of TNFα plus either purified sdAb-TNFα or *B. theta* culture supernatants containing sdAb-TNFα secreted by each of the 26 secretion carriers. Data are presented as the mean ± standard deviation of three biological samples for 26 secretion carriers and two biological samples for purified sdAb-TNFα. Source data are provided as a Source Data file.

https://doi.org/10.1038/s41467-024-53845-7

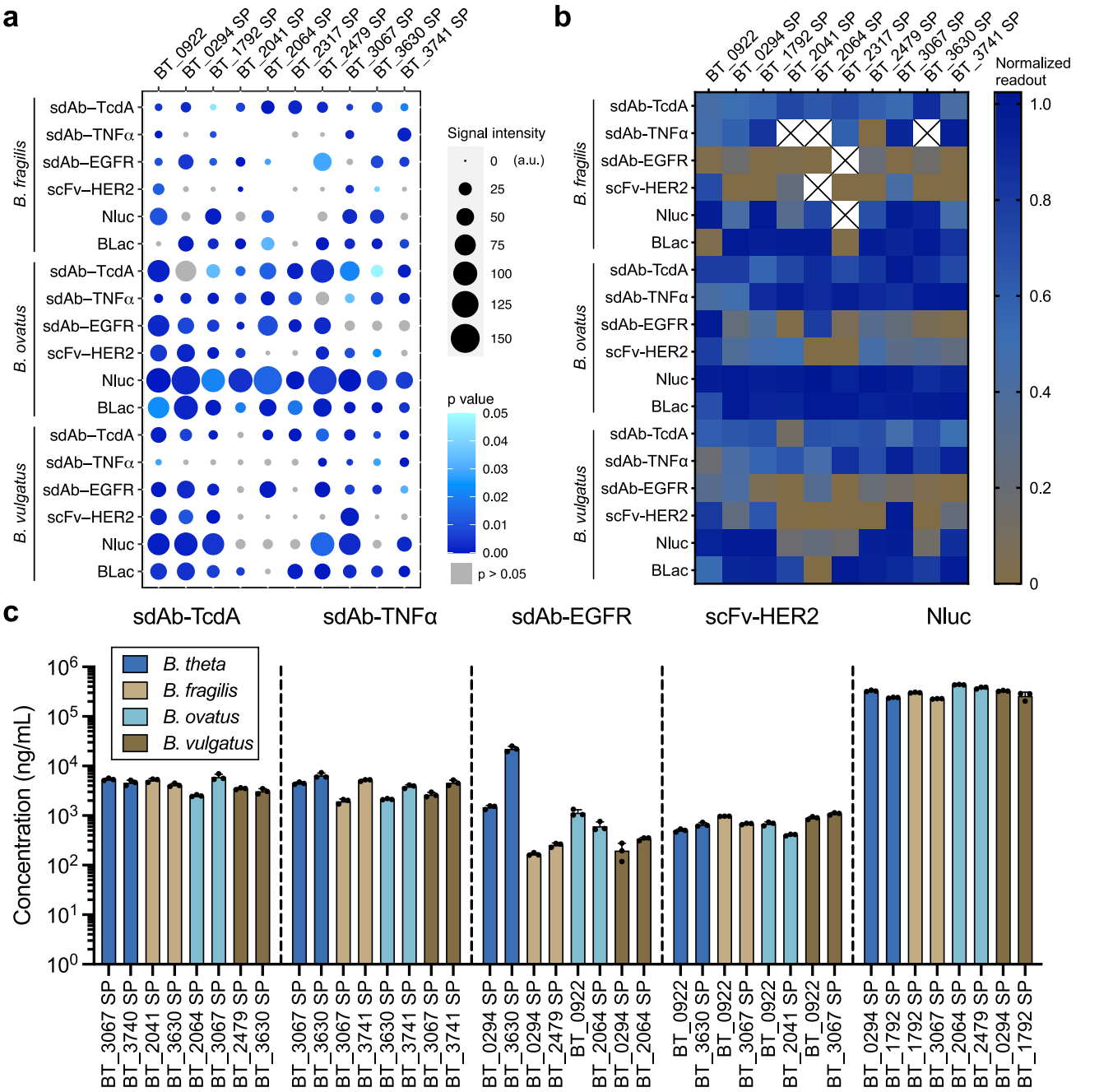

Fig. 4 | *B. theta*-derived secretion carriers mediate export of diverse, functional cargo proteins from multiple *Bacteroides* species. a Relative levels of six cargo proteins detected in the culture supernatants of three *Bacteroides* species, driven by each of the ten *B. theta*-derived secretion carriers with the highest functional secretion score. Bubble size corresponds to average dot blot signal intensity of three biological samples with $p < 0.05$ indicated by the blue color scale and $p > 0.05$ shown in gray. Significance was determined using unpaired two-tailed Welch's *t* test comparing to the culture supernatants of wild-type strains. **b** Functional assays of antibody fragments and reporter proteins secreted into culture supernatant of *B. fragilis*, *B. ovatus*, and *B. vulgatus* by *B. theta*-derived secretion carriers. Binding of antibody fragments (sdAb-TcdA, sdAb-TNFα, sdAb-EGFR, and scFv-HER2) to their respective targets was determined by ELISA. Enzymatic activity of reporter proteins (Nluc and BLac) was determined by bioluminescence or colorimetric assay, respectively. Following log transformation of luminescence data, all functional assay readouts were converted to values between zero and one by cargo-wise min-max normalization. All functional assays were performed with three biological replicates. **c** Quantitation of protein secretion titers mediated by the two secretion carriers that yielded the highest functional protein levels of each cargo in each species. Data are presented as the mean ± standard deviation of three biological samples. Source data are provided as a Source Data file.

ovatus[17]. As we observed with *B. theta*, Nluc generally had the highest secretion levels among the six cargo proteins across all three *Bacteroides* species. In contrast, efficient secretion of sdAb-EGFR and scFv-HER2 appears to be restricted to only a few selected secretion carriers.

After validating the heterologous protein secretion capability of the *B. theta*-derived secretion carriers across four *Bacteroides* species, we next sought to quantify secretion titers in these species. For these measurements, we selected five of our seven cargo proteins: four antibody fragments and the most robust reporter, Nluc. For each protein, we identified the two secretion carriers that yielded the highest functional secretion scores in each species (Fig. 4b) and selected these carrier-cargo-species combinations for our analysis.

https://doi.org/10.1038/s41467-024-53845-7

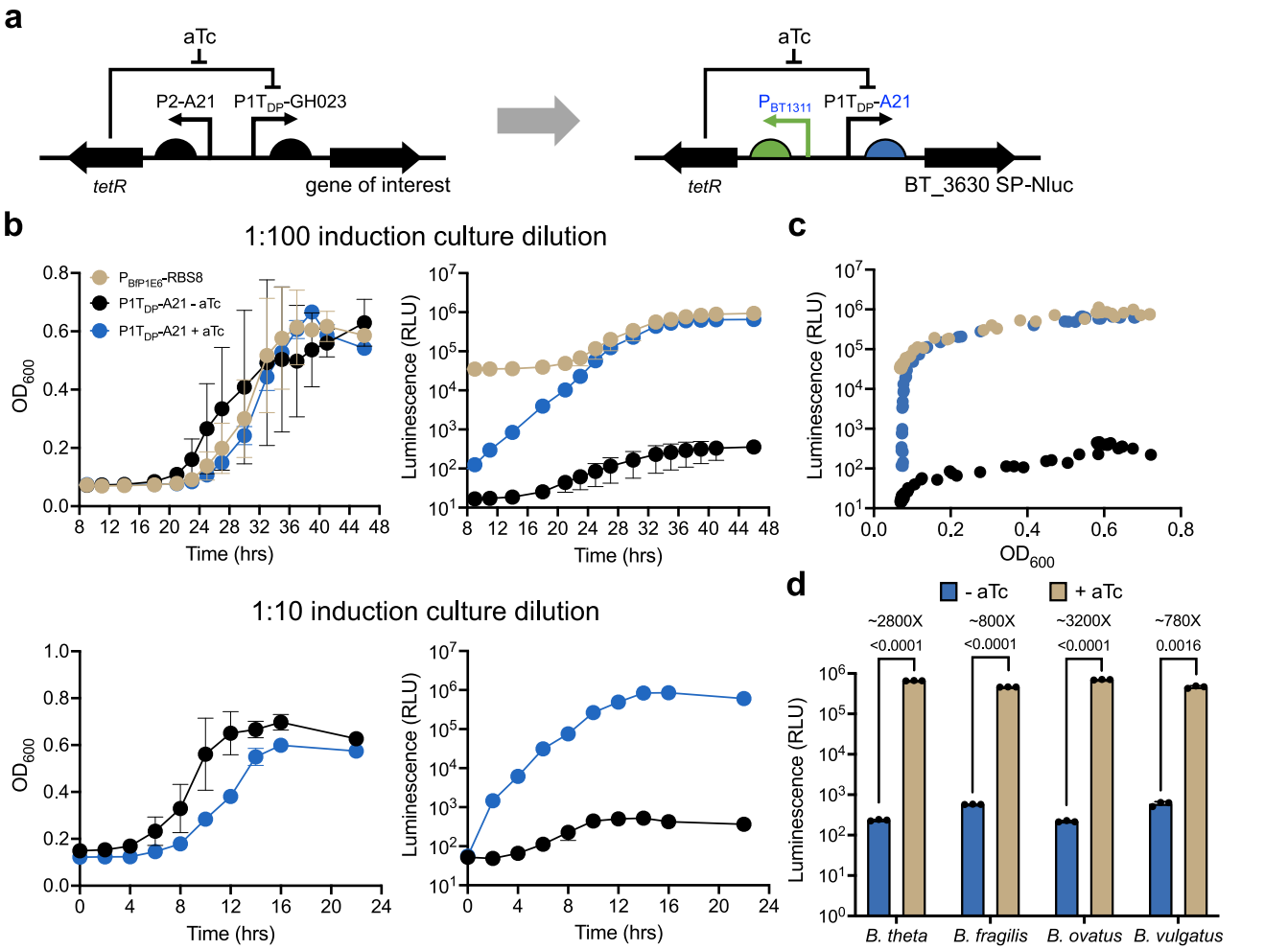

Fig. 5 | Development of a strong, aTc-inducible expression cassette for enhanced control of protein secretion across multiple *Bacteroides* species. **a** Low-activity promoter and RBS sequences in the original P2-A21-tetR-P1T$_{DP}$-GH023 inducible expression cassette (left)[17] were replaced with high-activity variants to generate the modified P$_{BT1311}$-tetR-P1T$_{DP}$-A21 expression cassette (right). **b** Modified inducible expression cassette drives expression of Nluc reporter at levels similar to high-level constitutive promoter P$_{BfP1E6}$-RBS8 in cultures diluted at 1:100 (top) or 1:10 (bottom). Data are presented as the mean ± standard deviation of three biological samples. **c** Correlation between bacterial growth and Nluc secretion levels shown in the top panel of Fig. 5b. **d** Modified inducible system mediates tightly controlled expression and secretion of BT_3630 SP-Nluc across multiple *Bacteroides* species. Data are presented as the mean ± standard deviation of three biological samples. Significance was determined using unpaired two-tailed Welch's *t* test. *P* values are reported in the figures. Source data are provided as a Source Data file.

Cultures were grown to late-log phase, and the concentration of secreted product in each culture supernatant was determined by comparison to standard curves of known concentrations of purified proteins (Fig. 4c). For the subset of secretion carriers tested, we observed comparable secretion titers across all four *Bacteroides* species, between 150-440000 ng/mL (Fig. 4c). Finally, to ensure that protein accumulation in culture supernatants was not the product of cell lysis, we performed western blot analysis to detect cargo proteins alongside GroEL, a housekeeping cytoplasmic protein that should not be present in the supernatant if cells remain intact. We analyzed cell pellets and supernatants from cultures of all *B. theta* strains shown in Fig. 4c (Supplementary Fig. 5a) as well as supernatants from cultures of the Nluc-secreting *B. fragilis*, *B. ovatus*, and *B. vulgatus* shown in Fig. 4c (Supplementary Fig. 5b) and observed no significant cell lysis.

Modified inducible expression system yields enhanced protein secretion

Having successfully established an approach to enable heterologous protein secretion from *B. theta* and other *Bacteroides* species, we next sought to engineer additional layers of flexibility, control, and enhancement using an inducible gene expression system. In our initial studies, we observed that the aTc-inducible P2-A21-tetR-P1T$_{DP}$-GH023 expression cassette resulted in much lower secretion than P$_{BfP1E6}$-RBS8 (Fig. 1b), presumably due to lower expression. To generate an inducible system capable of achieving much higher expression levels, and thus much higher secretion levels, we introduced two modifications aimed at enhancing activity. First, we replaced the GH023 RBS with the A21 RBS (Fig. 5a), which was previously identified as the strongest RBS tested amongst a collection of *Bacteroides* RBS sequences when paired with the P1T$_{DP}$ promoter[17]. Because the original construct already contained an A21 RBS sequence (Fig. 1a), we replaced the TetR-driving P2-A21 promoter/RBS with P$_{BT1311}$ and its native RBS (Fig. 5a) to avoid issues such as unwanted homologous recombination events between identical RBS sequences[78].

To measure the activity of our enhanced inducible expression system, we fused Nluc with the high-efficiency secretion carrier BT_3630 SP and generated two expression/secretion constructs: one driven by the aTc-inducible P1T$_{DP}$-A21 promoter, and one driven by the high-activity constitutive P$_{BfP1E6}$-RBS8 as both a positive control and reference point for high-level expression (Fig. 5b, top). To quantify

secretion, we induced freshly diluted (1:100) overnight cultures with 100 ng/mL aTc and performed bioluminescence measurements from 8 to 46 hr post-induction. Induction of Nluc expression from the enhanced $P1T_{DP}$-A21 promoter resulted in secretion levels up to 2000-fold higher than uninduced controls and only ~1.4-fold lower than the highly active P_{BfP1E6}-RBS8 constitutively expressed control (Fig. 5b, top). Because the *B. theta* cultures demonstrated a period of initial slow growth following a 1:100 dilution of the overnight cultures into fresh induction medium, we repeated the experiment using cultures diluted at 1:10. These samples achieved late-log phase growth after only 14 hr, compared to nearly 35 hr for the samples diluted at 1:100, but reached nearly the same maximal secretion levels (Fig. 5b, bottom), which suggests that the density of the culture does not affect the induction of this promoter. As we observed in our initial growth experiments (Fig. 1b), secretion levels are highly correlated with the growth phase of liquid cultures (Fig. 5c). Notably, we observed a growth delay of *B. theta* $P1T_{DP}$-A21 with aTc induction, which was more obvious with the 1:10 culture dilution (Fig. 5b, bottom), suggesting that this strong inducible promoter may impart some metabolic burden for *B. theta*. To verify the portability of this modified promoter, we repeated the experiments in the four other *Bacteroides* species and observed that the enhanced inducible expression system yields similar levels of secreted Nluc, and similar fold-induction levels compared to uninduced samples, across all four species tested (Fig. 5d). Interestingly, for *B. fragilis* and *B. vulgatus*, this promoter gave rise to slightly lower secretion levels in induced cultures and slightly higher expression leakage in uninduced cultures, resulting in overall lower fold-induction levels for these two species. This difference, similar to what we observed for overall secretion carrier performance across *Bacteroides* species (Fig. 4), may also be linked to their evolutionary distance from the other two species.

Different secretion carriers mediate distinct post-secretion extracellular fate of protein cargoes

Toward our goal of reproducibly delivering therapeutic proteins into specific physiological niches such as the gut lumen, we next sought to investigate the post-secretion extracellular fate of heterologous proteins exported using our platform. Because we expect OMV-associated proteins to have fundamentally different characteristics than freely soluble proteins, such as thermostability, protease resistance, bioavailability, and dissemination to other body sites[79], precise determination of the extracellular destination mediated by different secretion carriers is required to fully optimize our platform. Based on the high secretion levels and high sensitivity observed in earlier experiments, we selected Nluc as the secretion cargo for these studies. From our collection of twenty-six effective secretion carriers (Fig. 1e), we selected four candidates with diverse structures and different secretion strategies (Fig. 1c) for further investigation: BT_0169 and BT_0569 (fusion partner; full-length secretion carriers with Sec/SPI SPs); BT_0922 (fusion partner; full-length secretion carrier with lipoprotein SP); and BT_3630 SP (OMV; lipoprotein SP).

To determine the extracellular fate of Nluc when secreted by these four carriers, we grew late-log phase liquid cultures of *B. theta* expressing each carrier-Nluc fusion, separated the cell pellets (P) from the total supernatants (T), then further separated the total supernatants into the soluble (S) and insoluble OMV (O) fractions. Cell pellets were concentrated 2.5-fold and OMV fractions were concentrated 20-fold during the extraction process. We measured the Nluc protein abundance (Fig. 6a) and luminescence (Fig. 6b) in each fraction. Consistent with the differences in carrier-specific Nluc secretion efficiency observed in earlier experiments (Fig. 3), western blot analysis revealed that the majority of the BT_0169-Nluc and BT_0569-Nluc were retained in the cell pellets, whereas BT_0922-Nluc and BT_3630 SP-Nluc were mostly secreted, although with different abundances in different fractions. BT_0922-Nluc appeared to have been cleaved, showing a faint band at its expected molecular weight of ~60 kDa in the cell pellet and OMV fractions while only a smaller, ~23 kDa product was detected in all other culture fractions. In the luciferase assay we found that, after separating out the OMVs, the soluble fraction of BT_0169-Nluc accounted for ~80% of the luminescence observed in the total supernatant (Fig. 6b), suggesting that BT_0169-Nluc is mainly secreted in a freely soluble form. The luminescence signals of the OMV-free soluble fractions of BT_0569-Nluc, BT_0922-Nluc, and BT_3630 SP-Nluc account for ~50% of the total supernatant signal, suggesting that these three secretion carriers mediate extracellular export of freely soluble and OMV-bound cargoes in roughly equal proportions. However, the luminescence signal from the concentrated OMV fractions was substantially higher for BT_0569 than for the other three secretion carriers. Remarkably, BT_3630 SP-Nluc appeared in both soluble and OMV fractions, suggesting that lipoprotein SPs secrete heterologous proteins through not only OMV-dependent but also OMV-independent pathways, which has been reported previously[80–82], but, to best of our knowledge, never for lipoprotein SPs nor in *Bacteroides* species.

Next, we investigated the OMV-specific localization of two secretion carrier-Nluc fusions to further refine our ability to precisely implement therapeutic protein delivery with our engineered platform. We selected BT_0569 and BT_3630 SP as the secretion carriers for this study. Because BT_0569 has a Sec SP, it should be predominantly secreted into the periplasm through the Sec pathway. Conversely, BT_3630 SP is a lipoprotein SP which, in *E. coli*, can deliver protein cargoes to the inner leaflet of the OM through the localization of lipoprotein (Lol) pathway or the outer leaflet of the OM with additional secretion machinery[83]. Therefore, we predicted that BT_0569-Nluc should be packed into the OMV lumen and BT_3630 SP-Nluc should be anchored on the OMV membrane during the vesiculation process. We performed a proteinase K accessibility assay on OMV fractions isolated from liquid cultures of *B. theta* expressing BT_0569-Nluc and BT_3630 SP-Nluc (Fig. 6c). BT_0569-Nluc was highly resistant to degradation at both early (5 min) and late (30 min) timepoints across nearly all proteinase K concentrations tested, whereas BT_3630 SP-Nluc was much more sensitive to degradation at the higher proteinase K concentrations and over time. These results are consistent with our prediction and further imply that BT_3630 SP may anchor cargo proteins to the outer leaflet of the OMV membrane. Together these results suggest that the post-secretion fate (soluble, OMV surface, or OMV lumen) of protein cargoes can be controlled by careful selection of secretion carriers (Fig. 6d), which will allow more refined customization of *Bacteroides*-based in situ delivery systems for specific applications in the future.

Probing the size limit of lipoprotein SP-mediated protein secretion

To fully explore the capacity of *B. theta* for in situ delivery of protein-based therapeutics, we next wanted to determine if there is a limit on the size of the protein cargo that can be secreted by lipoprotein SPs with high functional secretion scores (Fig. 3b). We therefore selected BT_3630 SP as our representative SP and fused it to seven different cargo proteins—three endogenous *B. theta* proteins and four heterologous proteins—selected to cover a broad range of molecular weight: Nluc (25 kDa), cellulase (Cel; 41 kDa), BT_3686 (53 kDa), chitinase (ChiA; 68 kDa), BT_3703 (SusB; 88 kDa), β-galactosidase (LacZ; 122 kDa), and BT_3169 (148 kDa) (Fig. 6e). All constructs were fused with a C-terminal 3xFLAG tag to enable immunodetection. Cargo sizes listed above include the combined molecular weight of each protein plus the signal peptide and 3xFLAG tag. To minimize the metabolic burden and toxicity of constitutive high-level protein expression during the post-conjugation recovery and selection phase of growth, we used the aTc-inducible $P1T_{DP}$-A21 promoter instead of the constitutive P_{BfP1E6}-RBS8. Following growth in liquid culture to late log phase, we analyzed the culture supernatants for the presence of each secreted

https://doi.org/10.1038/s41467-024-53845-7

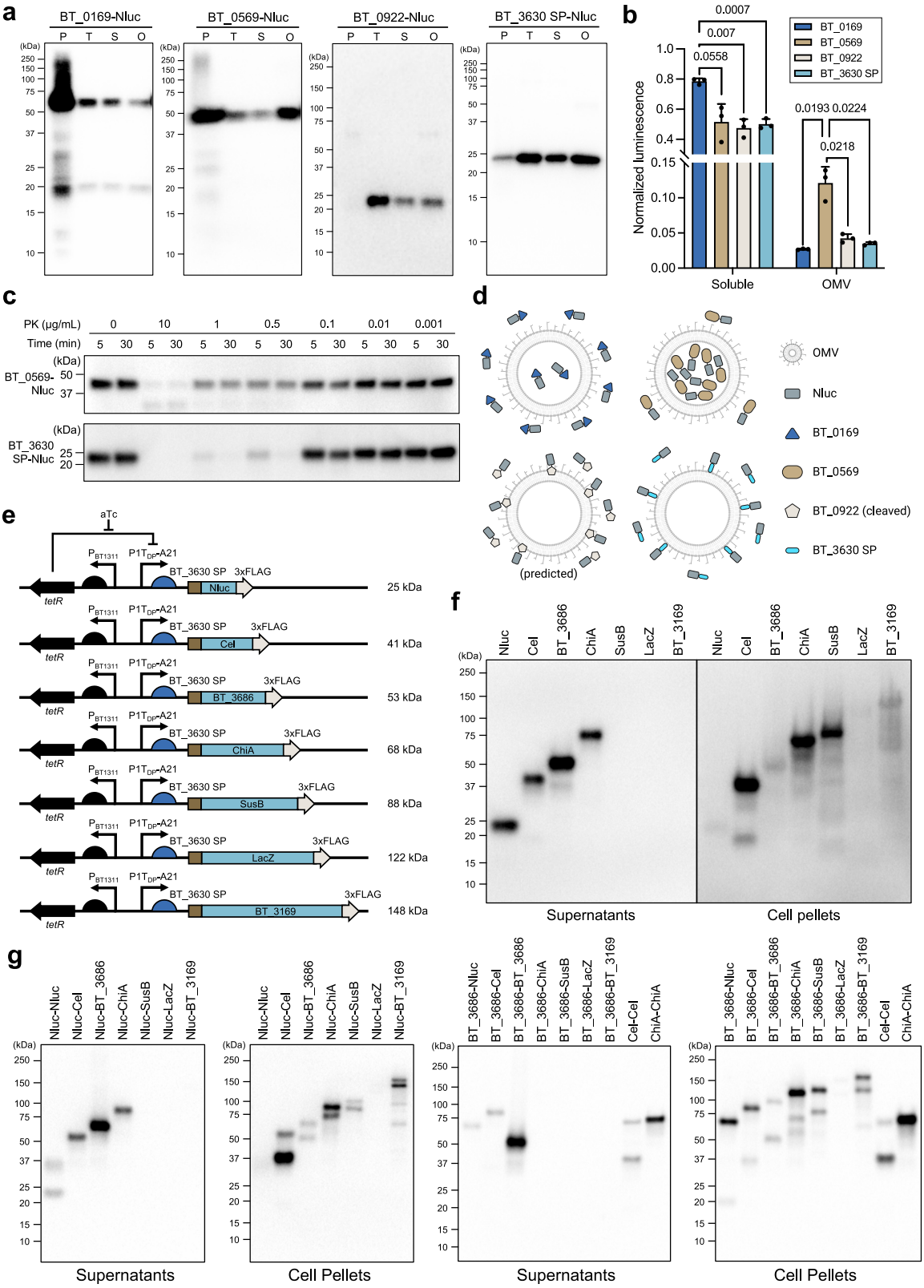

protein and only observed extracellular accumulation of the four smallest cargoes. The next largest protein cargo, SusB, was clearly observed in the pellet but not in the supernatant, suggesting a potential molecular weight cutoff between 68 and 88 kDa (Fig. 6f). To explore this further, we used the same proteins to generate a suite of fusions of varying size and analyzed their abundance in cell pellets and supernatants from *B. theta* culture (Fig. 6g). We detected two proteins in the supernatant that exceeded the previously identified putative molecular weight cutoff: Nluc-ChiA (87 kDa) and BT_3686-Cel (88 kDa). Proteins > 88 kDa were only detected in cell pellets, which may more accurately define the secretion size limit, but further investigation is needed to verify this.

Fig. 6 | Characterization of the post-secretion extracellular fate and size limit of secreted cargo proteins. a Western blot analysis of Nluc abundance in different fractions of *B. theta* liquid cultures expressing four carrier-Nluc constructs. P, cell pellet; T, total supernatant; S, soluble fraction of total supernatant; and O, OMV fraction of total supernatant. P and O fractions are 2.5-fold and 20-fold more concentrated than T and S fractions of equivalent volume, respectively. **b** Enzymatic activity of secreted Nluc in soluble and OMV fractions, measured by luminescence assay. To normalize the difference in Nluc secretion efficiency between the four secretion carriers, the luminescence in soluble and OMV fractions was divided by the luminescence in total supernatants to calculate the relative abundance of secreted Nluc in soluble and OMV fractions. Normalized luminescence of concentrated OMV fractions was divided by 20 to correct for concentration during sample prep. Data are presented as the mean ± standard deviation of three biological samples. Significance was determined using unpaired two-tailed Welch's *t* test. *P* values are reported in the figures. **c** Western blot analysis of proteinase K assay of OMV fractions from *B. theta* cultures expressing BT_0569-Nluc (Sec/SPI SP; predicted localization to OMV lumen) and BT_3630 SP-Nluc (lipoprotein SP; predicted localization to OMV surface). This experiment was performed with one biological replicate. PK, proteinase K **d** Schematic representation of post-secretion extracellular fate of Nluc mediated by BT_0169, BT_0569, and BT_3630 SP. BT_0922-Nluc is predicted to have a similar pattern as BT_3630 SP-Nluc as both have a lipoprotein SP and demonstrated similar abundance and localization in Figs. 7a and 7b. **e** Set of seven expression constructs generated to test the ability of BT_3630 SP to mediate secretion of different sized protein cargoes from *B. theta*. The molecular weight of each protein is shown on the right. **f** and **g** Western blot analysis of supernatants and cell pellets from the liquid culture of *B. theta* expressing seven proteins and their fusion proteins of varying size fused to BT_3630 SP. These experiments were performed with one biological replicate. Panel (**d**) Created in BioRender. Yeh, Y. (2023) BioRender.com/e26o022. Source data are provided as a Source Data file.

Secretion carriers mediate in situ delivery of heterologous proteins from *B. theta* in the mouse gut

To validate the in vivo functionality of our in vitro-characterized *B. theta* secretion carriers, we next investigated their performance in the gastrointestinal tract of mice. Following pre-treatment with an antibiotic cocktail, we orally gavaged C57BL/6 J mice with: *B. theta* constitutively expressing Nluc with no secretion carrier (intracellular control; no secretion), *B. theta* constitutively expressing Nluc fused with BT_0294 SP (plasmid pYHY1, high efficiency secretion; Fig. 4c and Supplementary Fig. 2), wild-type (WT) *B. theta* (negative control; no heterologous protein expression/secretion), or PBS (no treatment control) (Fig. 7a). We monitored general health (mouse weight), *B. theta* colonization (colony forming units [CFU] in feces), and Nluc activity (luminescence in feces) for sixty days (Fig. 7a). We observed no difference in weight between any group, suggesting that our engineered strains had no obvious adverse effects on mouse health (Fig. 7b). Both the intracellular and secreted Nluc strains engrafted and persisted at above 10^6 CFU/mg feces (Fig. 7c), despite a slow decrease from ~2×10^7 CFU/mg feces at day one to ~5×10^6 CFU/mg feces at day sixty, demonstrating robust, long-term colonization in antibiotic pre-treated mice.

Because we performed these studies in antibiotic-treated conventional mice rather than germ-free, we used selective plating to isolate and quantify fecal CFU of our strains, which harbor the erythromycin-resistance gene. Thus, the CFU of the WT strain, which has no erythromycin-resistance marker, could not be quantified using this approach (Fig. 7c). Luminescence activity for both intracellular and secreted Nluc was readily detectable in the feces over the entire experimental time course, indicating that the secreted cargo was not only continuously present but also functional (Fig. 7d). The presence of Nluc in the fecal pellets of the mice colonized with the non-secreting (intracellularly expressing) *B. theta* strain suggests that some cell lysis occurred either in the mouse intestine or ex vivo during sample processing; however, the fecal luminescence measurements from mice colonized with *B. theta* expressing BT_0294 SP-Nluc (secreted) were around ten-fold higher than the intracellular Nluc values throughout the experimental time course. To determine if the slow decrease over time that we observed in colonization and luminescence for both the intracellular and secreted Nluc variants (Fig. 7c, d) was due to plasmid loss in the absence of antibiotic selection pressure, we generated a BT_0294 SP-Nluc expression/secretion plasmid using pNBU1[22], which stably integrates into the genome. We repeated the in vivo study comparing colonization and luminescence of pYHY1 to pNBU1 *B. theta* strains (Fig. 7e–g), with or without plasmid-selective antibiotics added to the drinking water. Without antibiotic selection, Nluc secretion still decreased over time for both genomically integrated (pNBU1) and episomal (pYHY1) constructs (Fig. 7f), whereas antibiotic selection led to more stable and prolonged *B. theta* colonization (Fig. 7e) and Nluc secretion (Fig. 7f), suggesting that a lack of selective pressure promotes a general reduction in the abundance of engineered bacteria in the mouse gut that is not necessarily tied to plasmid loss. In addition, we calculated luminescence normalized to bacterial CFU, which remained largely consistent after the fifth day for all groups (Fig. 7g), indicating that the expression/secretion plasmids retained functionality and were likely not subject to mutational inactivation.

Discussion

Bacteroides species are a promising chassis for developing long-term interventions for diseases of the GI tract. However, the lack of efficient heterologous protein secretion tools for this genus limits their ability to serve as in situ production and delivery vehicles for therapeutic payloads or diagnostic reporters. In this work, we describe the development, characterization, and implementation of a molecular toolkit to enable efficient protein secretion in *Bacteroides* species. Previous studies attempting to address this need were able to achieve low levels (< 10 ng/mL) of secretion of a number of different heterologous proteins, including human keratinocyte growth factor-2 (hKGF-2)[15,40], murine interlukein-2 (mIL2)[38], and human transforming growth factor β1 (hTGF-β1)[39], using SP sequences derived from either *B. fragilis* enterotoxin (BFT)[15,38,39] or *B. theta* OmpA (BT_3852)[40]. A key finding of our current work is the identification and characterization of a collection of lipoprotein SP and full-length protein secretion carriers derived from endogenous *B. theta* secretory proteins that enable efficient secretion at titers of up to ~440 μg/mL of functional heterologous proteins from multiple *Bacteroides* species. Interestingly, the two *E. coli* secretion systems we tested did not function at all in *B. theta*. This is likely due to the phylogenetic distance between these two species, which is much larger than the distance between *Salmonella enterica* serovar Typhimurium and *E. coli*[84], for which successful secretion machinery swapping has been described[49]. Notably, several *Bacteroides* species are reported to have native T6SS and T9SS[36,37,85], which are potential targets for future engineering and development of novel secretion tools.

Beyond our primary goals of achieving highly efficient protein secretion and identifying the sequence determinants that promote this optimized performance, we also undertook a detailed exploration of our engineered platform by examining specific behaviors of the system and its components. Toward the goal of developing a fully characterized and flexible platform for diverse biomedical applications, we identified a size limit of 88 kDa as a potential cutoff for efficient secretion of heterologous proteins from *Bacteroides* species. While proteins larger than 88 kDa have been found in *Bacteroides* species-derived OMVs[42], they may require additional machinery for efficient secretion, such as the β-barrel translocator domain of the autotransporter system (T5SS)[41]. We also investigated the post-secretion extracellular fate of the heterologous protein cargo and identified differential secretion patterns depending on the secretion carrier. From these studies, we identified *B. theta* secretion carriers

https://doi.org/10.1038/s41467-024-53845-7

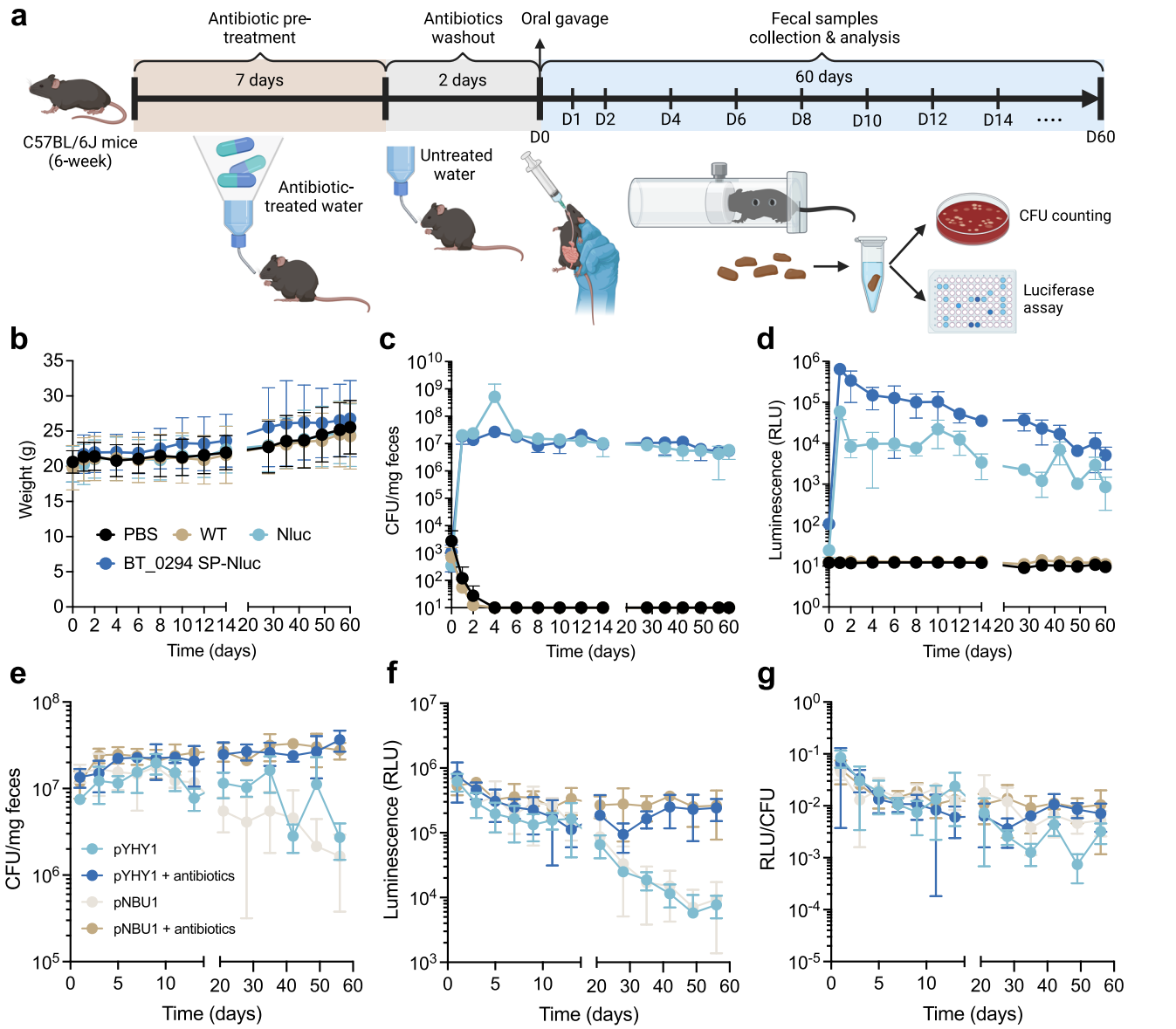

Fig. 7 | Direct intestinal delivery of heterologous protein cargo by *B. theta* in mice. a Design of in vivo experiments. Mice were monitored and fecal samples were collected and analyzed for sixty days following inoculation. **b** The weight of mice in all groups increased similarly over time, indicating no adverse health effects. **c** Engineered *B. theta* strains persisted at high levels in the mouse intestine, as determined by fecal CFU counts (limit of detection: 10 CFU/mg feces). **d** The functionality of intestinally delivered protein cargo (Nluc) persisted over time, as determined by luminescence measurements of fecal homogenates. **e**, **f**, and **g** The colonization (**e**), luminescence of Nluc in feces (**f**), and luminescence normalized by CFU (**g**) of the *B. theta* strain expressing secretory BT_0294 SP-Nluc. For all panels, data are presented as the mean ± standard deviation of the results of each group of mice ($n = 4$ mice per group; one mouse in the pNBU1 + antibiotics group died at D13, and one mouse in pYHY1 + antibiotics group died at D42). Panel (**a**) Created in BioRender. Yeh, Y. (2023) BioRender.com/h86o809. Source data are provided as a Source Data file.

that appear to preferentially export protein cargo freely into the extracellular space (BT_0169), packaged within the OMV lumen (BT_0569), or bound to the OMV surface (BT_3630 SP). These findings support multiple avenues for future development of living therapeutic interventions. For example, proteins that are freely secreted into the extracellular space can efficiently exceed the threshold concentration required for therapeutic efficacy over short distances, whereas proteins packed into the OMV lumen have higher thermostability and protease resistance, enabling long-distance dissemination in the GI tract[79]. Secretion of surface-bound antibody fragments or receptor ligands on the outside of OMVs could facilitate targeted delivery of OMV-based therapeutics[86,87]. OMVs are also able to enter antigen-presenting cells via endocytosis and induce immunogenic responses[79,88], highlighting a potential future application of our secretion tools for development of *Bacteroides*-derived OMV vaccines.

Similar post-secretion protein localization results were recently reported for *E. coli* Nissle 1917 in which the SP from the *E. coli* lipoprotein Lpp, truncated OmpA, or hemolysin ClyA were fused to cargo proteins to direct them toward the lumen or external surface of OMVs[89], suggesting that secretion machinery plays a key role in determining the localization of exported proteins on OMVs. Notably, the Lpp SP promoted anchoring of protein cargo to the OMV membrane within the lumen, whereas the SP of the *B. theta* lipoprotein BT_3630 exported membrane-anchored proteins to the external OMV surface. This suggests a possible dual-orientation distribution for lipoprotein SP-mediated anchorage on OMVs, similar to some lipoproteins on the OM[90,91]. In another recent study also using *E. coli* as a

model, cargo proteins fused with membrane proteins (OmpA, SLP, or SlyB), periplasmic proteins (BtuF or MBP), or a series of truncated Lpp SPs with different linkers demonstrated precisely controlled distribution and orientation in relation to OMVs[92]. Interestingly, the authors found that the size and number of OMVs produced by *E. coli* varied based on the fusion partner and fusion linker length, indicating a possible mechanism behind the cargo-dependent variability we observed with different secretion carriers in *Bacteroides* species. These features, together with the predicted size limit and post-secretion distribution that we observed, suggest that unknown lipoprotein transportation, sorting, and secretion systems exist in *Bacteroides*. Indeed, recent transposon mutagenesis studies in *B. theta* have revealed novel systems involved in OMV production[93,94], however, whether these systems are involved in lipoprotein sorting and protein packing into OMVs remains unclear and further investigation is required before these mechanisms can be exploited to improve secretion output.

The secretion carriers developed in this study enable enhanced heterologous protein secretion across multiple *Bacteroides* species. This platform expands the applicability of living therapeutics, which have previously focused largely on metabolic disorders and cancer in clinical development[4] and have relied heavily on transiently colonizing probiotic strains, such as *E. coli* Nissle 1917 and *Lactococcus lactis*. By establishing a toolbox enabling the secretion of biotherapeutic proteins from permanently colonizing *Bacteroides* strains, we provide a means to utilize the living therapeutics platform for a broader range of diseases, including chronic conditions that require continuous treatment. Our additional characterization of the secretion carriers that we identified also provides a means for downstream users to select or engineer secretion carriers that are best suited for their particular goals and applications. Building on the success of our enhanced tunable promoter, future refinement of this platform will include incorporation of more sophisticated gene circuits for more precise control of expression/secretion outputs[22], sense-and-respond circuits for disease-specific activation of therapeutic response[95–97], and stable engraftment[25] and biocontainment[24] of engineered strains within the GI niche. Beyond therapeutic applications, *Bacteroides* species are prominent and abundant representative members of the gut microbiota[98]; the secretion tools described here could also be implemented for studying interspecies interactions and microbiota-host crosstalk in the gut.

Methods

Bacterial strains and culture

Bacteroides thetaiotaomicron VPI-5482, *Bacteroides fragilis* NCTC 9343, *Bacteroides ovatus* ATCC 8483, and *Bacteroides vulgatus* ATCC 8482 were acquired from ATCC. *Bacteroides* species were anaerobically cultured at 37 °C in TYG medium[22], BHIS medium (Brain Heart Infusion Supplemented with 1 μg/mL menadione, 0.5 mg/mL cysteine, 0.2 mM histidine, 1.9 μM hematin) or on BHI agar with 10% horse blood (BHIB). *E. coli* strains were aerobically cultured in LB medium at 37 °C. *E. coli* DH5α was used for plasmid maintenance and *E. coli* RK231[99] was used to achieve plasmid transfer into *Bacteroides* strains via tri-parental mating. For pNBU1-based plasmids, *E. coli* S17-1 λ pir was used for plasmid maintenance and conjugation. Antibiotics were used when required at the following concentrations: ampicillin 100 μg/mL, kanamycin 50 μg/mL, gentamicin 25 μg/mL for liquid cultures and 200 μg/mL for agar plates, and erythromycin 12.5 μg/mL.

Identification and selection of secretion carriers for fusion partner and OMV strategies

Based on the reported label-free quantification values (LFQ) of each *B. theta* protein in IM, OM, OMVp, or SUP fractions[42], we calculated and ranked three different $\log_2$(ratio) values ($\log_2$[SUP/IM + OM+OMVp], $\log_2$[OMVp/IM + OM + SUP], and $\log_2$[SUP+OMVp/IM + OM]) for every detected *B. theta* protein to determine which proteins are highly secreted in the soluble fraction, insoluble OMV fraction, or both fractions (Supplementary Data 1). From these three categories, we selected fifty-seven secretory proteins (Supplementary Data 2) to serve as secretion carriers for the fusion partner and OMV strategies. The twenty-nine proteins in all three categories with a Sec/SPI SP and the single protein with a Tat/SPI SP were used as full-length secretion carriers in the fusion partner strategy based on the assumption that their extracellular export relies on protein domains other than just their SPs. In addition, four lipoproteins with high $\log_2$(SUP/IM + OM +OMVp) values were also used as full-length secretion carriers in the fusion partner strategy based on previous reports in *E. coli*[83] demonstrating that lipoprotein SPs are only responsible for anchoring proteins to the IM or OM, and other domains of the secreted protein may help mediate extracellular export in freely soluble form. For the remaining twenty-three lipoproteins with high $\log_2$[OMVp/IM + OM + SUP] or $\log_2$[SUP+OMVp/IM + OM], we identified the N-terminal charged and central hydrophobic regions preceding the cysteine cleavage site and used this along with ~20 additional amino acids following the cleavage site as the secretion carriers for the OMV strategy. BT_p548220 is a lipoprotein expressed from an endogenous *B. theta* plasmid and has a high $\log_2$(SUP+OMVp/IM + OM); it was selected as part of the OMV strategy due to its homology with a highly secreted *B. fragilis* plasmid-expressed protein, BF9343.20c[100]. BT_2472, though it has the highest $\log_2$(SUP/IM + OM+OMVp), was not selected because we could not detect its secretion after C-terminal fusion with 3xFLAG (Fig. 1b).

Molecular cloning

Q5 high-fidelity DNA polymerase (New England Biolabs) was used for PCR amplification of DNA fragments for cloning. All primers were synthesized by Integrated DNA Technologies (IDT). All plasmid construction was done by Gibson Assembly (HiFi DNA Assembly Master Mix, New England Biolabs) and validated by sequencing. Plasmids were stored in *E. coli* DH5α or *E. coli* S17-1 λ pir for maintenance and conjugation. To increase protein expression levels in *Bacteroides* species, we constructed an episomal *E. coli-Bacteroides* shuttle vector, pYHY1 (Addgene Plasmid #215926) via Gibson assembly. All endogenous secretion carriers were cloned from the genome of *B. theta*. The HlyA, HlyB, HlyD of UPEC T1SS were cloned from pVDL9.3 (Addgene Plasmid #168299) and pEHlyA5 (Addgene Plasmid #168298) plasmids. The CsgG of *E. coli* K-12 T8SS was cloned from the genome of *E. coli* DH5α. For constructs with short N-terminal fusions (CsgA [N-terminal 22 residues], SusB SP, BT_3769 SP, and BFT SP), the sequences were introduced at the N-terminus of cargo proteins directly through overhang PCR. The sequences of P_{BfP1E6}, sdAb-TcdA, sdAb-TNFα, scFv-HER2, and EGFP were synthesized by IDT. The sequences of Nluc and sdAb-EGFR were cloned from plasmids pNBU2_erm-TetR-P1T_DP-GH023-NanoLuc (Addgene Plasmid #117728) and pTrcHIS-wt7D12 (Addgene Plasmid #125268). All promoters, RBS, secretion carriers, and protein cargoes were cloned into pYHY1 vector at the sequence between *ampR* and *ermG*. A 3xFLAG tag and the rrnb T1 terminator of *E. coli* were introduced at the 3'end of the protein coding region by PCR. A GSSG or GSSGSSG linker was introduced at the C-terminus of each protein, in frame with the 3xFLAG tag and a GSGGSGSSGS linker was introduced at C-terminus of each full-length secretion carrier, in frame with the protein cargo, by PCR. For plasmids used for recombinant protein expression and purification, the toxin A fragment (TcdAf; amino acid residues 2460-2710) was amplified from the *C. difficile* genome by PCR and cloned into the 2Bc-T plasmid (Addgene Plasmid #37236); 3xFLAG tagged Nluc, sdAb-TcdA, sdAb-TNFα, and sdAb-EGFR as well as untagged scFv-HER2 were cloned into the pET24b(+) plasmid with an N-terminal fusion with the *E. coli* outer membrane protein A (OmpA) signal peptide to for secretion of proteins into the periplasm[101].

Conjugation and selection

Plasmids for *Bacteroides* conjugations were first used to transform *E. coli* DH5α or *E. coli* S17-1 λ pir to generate plasmid donor *E. coli* strains. Equal volumes of overnight cultures of plasmid donors, *E. coli* RK231 (tri-parental mating helper strain), and *Bacteroides* (plasmid recipient) were spun down and washed once with PBS. For each conjugation, the cell pellet of the donor, recipient, and helper (if needed) were serially resuspended in 30 μL PBS, spotted onto BHIB plates, and incubated aerobically overnight at 37 °C upside down (lid on top). Mating spots were scraped off of plates, streaked onto BHIB plates supplemented with 200 μg/mL gentamicin and 12.5 μg/mL erythromycin, and incubated anaerobically for 2–3 days at 37 °C to allow selective growth of transconjugant *Bacteroides* clones.

Recombinant protein expression and purification

For sdAb-TcdA and toxin A fragment (TcdAf) purification, an overnight culture of *E. coli* BL21(DE3) harboring the 2Bc-T-TcdAf plasmid was grown overnight at 37 °C with shaking, then diluted 50-fold in 50 mL terrific broth (yeast extract 24 g, tryptone 20 g, glycerol 4 mL, 100 mL KPO_4 buffer [0.17 M KH_2PO_4, 0.72 M K_2HPO_4] per liter of medium) with 50 μg/mL kanamycin. When culture OD_{600} reached 0.6, isopropyl β-D-thiogalactoside (IPTG) was added to a final concentration of 0.1 mM to induce protein expression. After overnight induction of cultures at 25 °C with shaking, the cells were harvested and sonicated in lysis buffer (20 mM sodium phosphate, 0.5 M NaCl, 40 mM imidazole, 1% Triton X100, 0.1 mM PMSF pH 7.4). The soluble fractions of cell lysates were passed through a Ni-NTA chromatography column, and the recombinant TcdAf proteins were eluted with elution buffer (20 mM sodium phosphate, 0.5 M NaCl, and 500 mM imidazole). The concentration of purified TcdAf was calculated from A280, molecular weight, and extinction coefficient using the Beer-Lambert law. For Nluc, sdAb-TcdA, sdAb-TNFα, and sdAb-EGF, the expression plasmids were introduced into *E. coli* BL21(DE3). Overnight cultures of *E. coli* BL21(DE3) in LB were diluted 50-fold in 100 mL BHI with 50 μg/mL kanamycin. After the OD_{600} reached 0.3, protein expression was induced with 0.1 mM IPTG and cultures were grown overnight with shaking at 27 °C for sdAb-TcdA, sdAb-TNFα, and sdAb-EGFR and at 22 °C for Nluc. Cells were pelleted by centrifugation at 5000 × *g* for 10 min and sonicated in lysis buffer (PBS with 1% Triton X-100 and 0.1 mM PMSF). The soluble fraction of cell lysates was loaded on a column with anti-FLAG® M2 affinity gel (Sigma-Aldrich) for protein purification following the manufacturer's instructions. Untagged scFv-HER2 was purified from *E. coli* BL21(DE3) through the HiTrap™ Protein L column (Cytiva). The column was washed with PBS and the protein was eluted with 0.1 M glycine (pH 3.5). Protein concentration was determined by DC protein assay (Bio-Rad).

Immunoblot analysis of proteins

Bacteroides strains streaked on selective BHIB plates were inoculated into TYG or BHIS media with 25 μg/mL gentamicin and 12.5 μg/mL erythromycin (with 100 ng/mL aTc when using aTc-inducible promoters). After reaching late-log or stationary phase, culture supernatants were separated from bacterial cells by centrifugation at 10,000 × *g* for one minute and filtered through 0.22 μm PVDF syringe filters. For dot blot analysis, 10–30 μL of filtered supernatant was directly spotted onto a wet PVDF membrane placed on a stack of paper towels to aid rapid and consistent wicking of the samples through the membrane. For western blot analysis, 10.5 μL of filtered supernatant was mixed with 1.5 μL β-mercaptoethanol and 3 μL 5x sample loading buffer (300 mM Tris-HCl at pH 6.8, 10% SDS, 50% glycerol, and 0.5% bromophenol blue dye) and boiled at 98 °C for 10 min. 10 μL of boiled sample was subjected to Tris-glycine SDS-PAGE (12% gel or 4–20% gradient gel) in electrophoresis buffer (25 mM Tris-base, 250 mM glycine, and 0.1% SDS) at 100 V for 1.5 hr for protein separation. To analyze intracellular proteins, cell pellets from 0.5 mL liquid culture were washed once with PBS and resuspended in 50 μL 1x BugBuster protein extraction reagent (Merck Millipore). After 1 hr shaking at room temperature, PBS was added into cell lysates to a final volume of 0.5 mL, and 10.5 μL of cell lysate was processed and subjected to SDS-PAGE. Proteins were transferred to a PVDF membrane at 100 V for 1 hr in transfer buffer (25 mM Tris-base, 192 mM glycine, and 30% methanol). For both dot blots and westerns, the membranes were blocked with 5% milk in 0.1% PBS-T (phosphate-buffered saline with 0.1% Tween 20) at room temperature for 1 hr, then incubated with anti-FLAG M2 monoclonal antibody (Sigma-Aldrich, F1804, 1:2000 dilution in 5% milk/0.1% PBS-T) or anti-GroEL polyclonal antibody (Sigma-Aldrich, G6532, 1:5000 dilution in 5% milk/0.1% PBS-T) at 4 °C with rocking overnight. After washing three times with PBS-T, the membrane was incubated with goat anti-mouse IgG secondary antibody conjugated with horse radish peroxidase (HRP) (Jackson Immuno Research, 115-035-146, 1:5000 dilution in 5% milk/0.1% PBS-T) or goat anti-rabbit IgG-HRP (Invitrogen, 65–6120; 1:3000 dilution in 5% milk) at room temperature for 1 hr. Signal was detected using SuperSignal™ West Dura Extended Duration Substrate (Thermo Scientific) on a Bio-Rad GelDoc imaging system. For dot blot, the signal intensity was quantified by ImageJ. Briefly, the dot blot image was first inverted to obtain a black background, and the signal intensity of each dot was determined by calculating the mean gray value in the circular selection area via ROI Manager.

Measurement of activities of secreted antibody fragments and reporters in culture supernatants

Activity is defined as antigen binding for antibody fragments and enzymatic or fluorescent activity for reporter enzymes. The activities of all antibody fragments were measured by ELISA as follows: 96-well Immulon 2HB ELISA plates were coated with 1–2 μg/mL purified antigens (TcdAf, purified as described above; TNFα soluble form [#10602-HNAE-100], EGFR ECD [#10001-H08H], and HER2 ECD [#10004-H08H] were purchased from Sino Biological) at 4 °C overnight. After washing 3x with 0.1% PBS-T, plates were blocked with 5% milk/0.1% PBS-T for 1 hr at room temperature and washed again. Filtered culture supernatants (100 μL) or cell lysates (100 μL, processed as mentioned in immunoblot section) were added to wells and incubated for 1 hr at room temperature. Plates were washed again and anti-FLAG M2 antibody (Sigma-Aldrich, F1804, 1:2000 dilution in 5% milk/0.1% PBS-T) was added and incubated for 1 hr at room temperature. Following PBS-T washing, goat anti-mouse IgG secondary antibody conjugated with HRP (Jackson Immuno Research, 115-035-146, 1:5000 dilution in 5% milk/0.1% PBS-T) was added and incubated for 1 hr at room temperature. For scFv-HER2, protein L-HRP (VWR, PI32420, 1:5000 dilution in 5% milk/0.1% PBS-T) was used instead for detection. After washing with PBS-T, o-phenylenediamine (OPD) substrate solution was added and shaken for 10 min at room temperature. The absorbance at 450 nm (A450) was measured using a BioTek Synergy HT multimode microplate reader. To quantify secreted sdAb-TcdA, sdAb-TNFα, sdAb-EGFR, and scFv-HER2, 10-fold serially diluted purified proteins were run in parallel as standards, and the four-parameter logistic (4PL) regression model was applied to build the sigmoidal standard curves to estimate the secretion titer by GraphPad Prism 10. For NanoLuc, the Nano-Glo luciferase assay (Promega) was performed as follows: 5-10 μL undiluted or 10-fold diluted culture supernatant and cell lysate (processed as mentioned in immunoblot section) was mixed with 15–20 μL PBS, followed by mixing with 25 μL Nano-Glo® luciferase assay buffer supplemented with furimazine substrate at a ratio of 1:50. Luminescence was measured on the microplate reader using an integration time of 1 s and gain of 100. Quantification of secreted Nluc was achieved with a 10-fold serial dilution of purified 3xFLAG tagged Nluc and a standard linear regression model was applied to log-transformed luminescence (RLU) and concentration to build the standard curve for quantifying secreted Nluc. For β-lactamase, the β-lactamase activity assay kit (Sigma-

Aldrich) was used following the manufacturer's protocol. Briefly, 10 μL filtered culture supernatant was mixed with 40 μL PBS, followed by mixing with 50 μL β-lactamase assay buffer supplemented with nitrocefin substrate at a ratio of 1:25. Plates were incubated for 5 min at room temperature, then the absorbance at 490 nm (A490) was measured using the microplate reader.

Analysis of the post-secretion extracellular fate of secreted proteins

B. theta colonies were inoculated into 30 mL TYG with 12.5 μg/mL erythromycin and anaerobically grown to late log or stationary phase. 1 mL of liquid culture was first centrifuged at 10,000 × *g* for 1 min to separate cell pellets and culture supernatant. Cell pellets were then washed once with PBS to obtain the cell pellet fraction, which was then resuspended in 200 μL 2x sample loading buffer with 10% β-mercaptoethanol, boiled at 98 °C for 10 min, and diluted with 200 μL PBS to bring the sample buffer to 1x. The remaining 29 mL of culture was centrifuged at 5000 × *g* for 10 min to separate the cells and supernatant, and the supernatant was filtered through a 0.22 μm syringe filter to remove remaining cells and debris to obtain the cell-free total supernatant fraction. OMVs in the total supernatant fraction were extracted using the ExoBacteria™ OMV Isolation Kit (System Biosciences) according to the manufacturer's protocol: 25 mL of the total supernatant fraction was transferred to an OMV-binding column and rotated at 4 °C for 30 min. The column was uncapped, and the flow-through was collected as the OMV-free soluble fraction; finally, the column was washed twice with 15 mL binding buffer, and the OMVs were eluted with 1.25 mL elution buffer to obtain the 20x-concentrated OMV fraction. For western blot analysis, 10.5 μL from the total supernatant, soluble, and OMV fractions were mixed with 1.5 μL β-mercaptoethanol and 3 μL 5x sample loading buffer and boiled at 98 °C for 10 min. SDS-PAGE and immunoblotting were performed as described above with 10 μL of each processed fraction. For Nluc quantification, 10 μL of total supernatant, soluble, and OMV fractions containing secreted Nluc were analyzed using the Nano-Glo assay as described above.

Proteinase K accessibility assay

The extracted OMV fractions (19 μL) from the culture supernatants of *B. theta* expressing BT_0569-Nluc or BT_3630 SP-Nluc were mixed with 1 μL diluted proteinase K solution to the final concentrations indicated in Fig. 6c and incubated at 37 °C for 5 min or 30 min. After incubation, 10.5 μL of mixture was immediately mixed with 1.5 μL β-mercaptoethanol and 3 μL 5x sample loading buffer and boiled at 98 °C for 10 min, then 10 μL of each boiled sample was subjected to SDS-PAGE and immunoblotting, performed as described above.

Analysis of size limit of lipoprotein SP-mediated protein secretion

Cellulase (Cel) and chitinase (ChiA) were cloned from pCellulose (Addgene Plasmid #36300), pET16better_H10_HRV3C_chitinase (Addgene Plasmid #175091). BT_3686, BT_3703 (SusB), and BT_3169 were cloned from the genome of *B. theta*. β-galactosidase (LacZ) was cloned from the genome of *E. coli* BL21(DE3). Homodimers and heterodimers were constructed via Gibson assembly. Gene expression was driven by the $P1T_{DP}$-A21 promoter on the pYHY1 vector, and plasmids were conjugated into *B. theta*. The transconjugant colonies of *B. theta* strains harboring these plasmids were inoculated into BHIS medium with 100 ng/mL aTc, 25 μg/mL gentamicin, and 12.5 μg/mL erythromycin and incubated anaerobically overnight. After reaching late log or stationary phase, cell pellets and supernatants from liquid cultures were processed and subjected to western blot analysis as described above.

TNFα neutralization assay

The murine L929 cell line (ATCC CCL-1) was used for measuring the neutralizing capacity of sdAb-TNFα secreted from *B. theta*. L929 cells were seeded in a 96-well plate with 1×10^4 cells in 100 μL DMEM per well and incubated at 37 °C overnight. Treatment mixtures for each well were generated by pre-incubating 100 μL of *B. theta* culture supernatants or serially diluted sdAb standards with 100 μL fresh DMEM containing 1 μg/mL actinomycin D and 4 ng/mL human TNFα for 1 hr at 37 °C. The mixtures were then used to replace the culture media of the L929 cells. After incubation at 37 °C for 20 hr, the viability of L929 cells was measured by MTT assay (Abcam) following the manufacturer's instructions.

In vivo Nluc secretion

All animal experiments were performed using protocols approved by the University of Illinois Institutional Animal Care and Use Committee. Mice were maintained at 22–26 °C, 30–70% humidity, and a 12-h light cycle. C57BL/6 J specific-pathogen-free (SPF) mice (6-8 weeks old; sex-balanced) were pre-treated with an antibiotic cocktail in their drinking water (1 g/L metronidazole, 1 g/L neomycin, 0.5 g/L vancomycin, and 1 g/L ampicillin, and 20 g/L Kool-Aid Drink Mix[102]) for 7 days followed by a 2-day washout period with plain tap water. Mice were divided into four groups (2 males and 2 females per group) and orally administered 200 μL of PBS or bacterial strains (1×10^9 CFU). Mice were weighed and fecal samples were collected every two days for two weeks, then once per week for another six weeks, with a final sample collected on day 60. For antibiotic water groups, mice were treated with 12.5 μg/mL erythromycin and 100 μg/mL gentamicin in their drinking water throughout the experiment. To quantify colonization of the engineered *B. theta* strains, fecal samples were homogenized in PBS (10 μL per mg of feces) and serially diluted in 96-well plates. Dilutions were plated on selective BHIB plates using a multi-channel pipettor and the highest dilution with single colonies was used to calculate CFU per mg of feces. To measure the level of secreted Nluc in fecal pellets, the homogenized fecal pellets were centrifuged at 12,000 × *g* for 2 min to pellet bacterial cells, then 25 μL of supernatant was used in the Nano-Glo luciferase assay described above.

Reporting summary

Further information on research design is available in the Nature Portfolio Reporting Summary linked to this article.

Data availability

The following plasmids, with maps and sequences, are available through Addgene: pYHY1 (empty *E. coli-Bacteroides* shuttle vector; Addgene Plasmid #215926), pYHY2 (pYHY1-P_{BfP1E6}-RBS8-BT_0294 SP-Nluc-3xFLAG; Addgene Plasmid #216108), and pYHY3 (pYHY1-P_{BT131I}-tetR-$P1T_{DP}$-A21-BT_3630 SP-Nluc-3xFLAG; Addgene Plasmid #216109). Source data are provided with this paper.

References

1. Kelly, V. W., Liang, B. K. & Sirk, S. J. Living therapeutics: the next frontier of precision medicine. *ACS Synth. Biol.* **9**, 3184–3201 (2020).
2. Pedrolli, D. B., Ribeiro, N. V., Squizato, P. N., de Jesus, V. N. & Cozetto, D. A. Engineering microbial living therapeutics: the synthetic biology toolbox. *Trends Biotechnol.* **37**, 100–115 (2019).
3. Isabella, V. M. et al. Development of a synthetic live bacterial therapeutic for the human metabolic disease phenylketonuria. *Nat. Biotechnol.* **36**, 857–864 (2018).
4. Charbonneau, M. R., Isabella, V. M., Li, N. & Kurtz, C. B. Developing a new class of engineered live bacterial therapeutics to treat human diseases. *Nat. Commun.* **11**, 1738 (2020).

5. Chen, Z. et al. Incorporation of therapeutically modified bacteria into gut microbiota inhibits obesity. *J. Clin. Invest* **124**, 3391–3406 (2014).
6. Somabhai, C. A., Raghuvanshi, R. & Nareshkumar, G. Genetically engineered escherichia coli nissle 1917 synbiotics reduce metabolic effects induced by chronic consumption of dietary fructose. *PLoS One* **11**, e0164860 (2016).
7. Steidler, L. et al. Treatment of murine colitis by lactococcus lactis secreting interleukin-10. *Science* **289**, 1352–1355 (2000).
8. Zhang, Y. et al. Escherichia coli Nissle 1917 targets and restrains mouse B16 melanoma and 4T1 breast tumors through expression of azurin protein. *Appl Environ. Microbiol* **78**, 7603–7610 (2012).
9. Hwang, I. Y. et al. Engineered probiotic Escherichia coli can eliminate and prevent Pseudomonas aeruginosa gut infection in animal models. *Nat. Commun.* **8**, 15028 (2017).
10. Ho, C. L. et al. Engineered commensal microbes for diet-mediated colorectal-cancer chemoprevention. *Nat. Biomed. Eng.* **2**, 27–37 (2018).
11. Palmer, J. D. et al. Engineered Probiotic for the Inhibition of Salmonella via Tetrathionate-Induced Production of Microcin H47. *ACS Infect. Dis.* **4**, 39–45 (2018).
12. Consortium, T. H. M. P. Structure, function and diversity of the healthy human microbiome. *Nature* **486**, 207–214 (2012).
13. Wexler, H. M. Bacteroides: the good, the bad, and the nitty-gritty. *Clin. Microbiol Rev.* **20**, 593–621 (2007).
14. Faith, J. J. et al. The long-term stability of the human gut microbiota. *Science* **341**, 1237439 (2013).
15. Hamady, Z. Z. et al. Xylan-regulated delivery of human keratinocyte growth factor-2 to the inflamed colon by the human anaerobic commensal bacterium Bacteroides ovatus. *Gut* **59**, 461–469 (2010).
16. Jones, D. R. et al. Engineering dual-glycan responsive expression systems for tunable production of heterologous proteins in Bacteroides thetaiotaomicron. *Sci. Rep.* **9**, 17400 (2019).
17. Lim, B., Zimmermann, M., Barry, N. A. & Goodman, A. L. Engineered regulatory systems modulate gene expression of human commensals in the gut. *Cell* **169**, 547–558.e515 (2017).
18. Mimee, M., Tucker, A. C., Voigt, C. A. & Lu, T. K. Programming a human commensal bacterium, Bacteroides thetaiotaomicron, to sense and respond to stimuli in the murine gut microbiota. *Cell Syst.* **2**, 214 (2016).
19. Whitaker, W. R., Shepherd, E. S. & Sonnenburg, J. L. Tunable expression tools enable single-cell strain distinction in the gut microbiome. *Cell* **169**, 538–546.e512 (2017).
20. García-Bayona, L., and Comstock, L. E. Streamlined genetic manipulation of diverse bacteroides and parabacteroides isolates from the human gut microbiota. mBio *10*. https://doi.org/10.1128/mBio.01762-19 (2019).
21. Horn, N. et al. A novel tightly regulated gene expression system for the human intestinal symbiont Bacteroides thetaiotaomicron. *Front Microbiol* **7**, 1080 (2016).
22. Taketani, M. et al. Genetic circuit design automation for the gut resident species Bacteroides thetaiotaomicron. *Nat. Biotechnol.* **38**, 962–969 (2020).
23. Zheng, L. et al. CRISPR/CAS-based genome editing for human gut commensal Bacteroides species. *ACS Synth. Biol.* **11**, 464–472 (2022).
24. Wegmann, U., Carvalho, A. L., Stocks, M. & Carding, S. R. Use of genetically modified bacteria for drug delivery in humans: Revisiting the safety aspect. *Sci. Rep.* **7**, 2294 (2017).
25. Shepherd, E. S., DeLoache, W. C., Pruss, K. M., Whitaker, W. R. & Sonnenburg, J. L. An exclusive metabolic niche enables strain engraftment in the gut microbiota. *Nature* **557**, 434–438 (2018).
26. Riglar, D. T. & Silver, P. A. Engineering bacteria for diagnostic and therapeutic applications. *Nat. Rev. Microbiol* **16**, 214–225 (2018).
27. Sieow, B. F., Wun, K. S., Yong, W. P., Hwang, I. Y. & Chang, M. W. Tweak to treat: reprograming bacteria for cancer treatment. *Trends Cancer* **7**, 447–464 (2021).
28. Anné, J., Economou, A. & Bernaerts, K. Protein secretion in gram-positive bacteria: from multiple pathways to biotechnology. *Curr. Top. Microbiol Immunol.* **404**, 267–308 (2017).
29. Schneewind, O. & Missiakas, D. M. Protein secretion and surface display in Gram-positive bacteria. *Philos. Trans. R. Soc. Lond. B Biol. Sci.* **367**, 1123–1139 (2012).
30. Costa, T. R. et al. Secretion systems in Gram-negative bacteria: structural and mechanistic insights. *Nat. Rev. Microbiol* **13**, 343–359 (2015).
31. Trivedi, A., Gosai, J., Nakane, D. & Shrivastava, A. Design principles of the rotary type 9 secretion system. *Front Microbiol* **13**, 845563 (2022).
32. Eom, G. T. et al. Efficient extracellular production of type I secretion pathway-dependent Pseudomonas fluorescens lipase in recombinant Escherichia coli by heterologous ABC protein exporters. *Biotechnol. Lett.* **36**, 2037–2042 (2014).
33. Bartra, S. S., Jackson, M. W., Ross, J. A. & Plano, G. V. Calcium-regulated type III secretion of Yop proteins by an Escherichia coli hha mutant carrying a Yersinia pestis pCD1 virulence plasmid. *Infect. Immun.* **74**, 1381–1386 (2006).
34. Akeda, Y. et al. Functional cloning of Vibrio parahaemolyticus type III secretion system 1 in Escherichia coli K-12 strain as a molecular syringe. *Biochem Biophys. Res Commun.* **427**, 242–247 (2012).
35. Lynch, J. P. et al. Engineered Escherichia coli for the in situ secretion of therapeutic nanobodies in the gut. *Cell Host Microbe* **31**, 634–649.e638 (2023).
36. Abby, S. S. et al. Identification of protein secretion systems in bacterial genomes. *Sci. Rep.* **6**, 23080 (2016).
37. Zafar, H. & Saier, M. H. Jr. Comparative genomics of transport proteins in seven Bacteroides species. *PLoS One* **13**, e0208151 (2018).
38. Farrar, M. D. et al. Engineering of the gut commensal bacterium Bacteroides ovatus to produce and secrete biologically active murine interleukin-2 in response to xylan. *J. Appl Microbiol* **98**, 1191–1197 (2005).
39. Hamady, Z. Z. et al. Treatment of colitis with a commensal gut bacterium engineered to secrete human TGF-β1 under the control of dietary xylan 1. *Inflamm. Bowel Dis.* **17**, 1925–1935 (2011).
40. Carvalho, A. L. et al. Bioengineering commensal bacteria-derived outer membrane vesicles for delivery of biologics to the gastrointestinal and respiratory tract. *J. Extracell. Vesicles* **8**, 1632100 (2019).
41. Burdette, L. A., Leach, S. A., Wong, H. T. & Tullman-Ercek, D. Developing gram-negative bacteria for the secretion of heterologous proteins. *Micro Cell Fact.* **17**, 196 (2018).
42. Valguarnera, E., Scott, N. E., Azimzadeh, P., and Feldman, M. F. Surface exposure and packing of lipoproteins into outer membrane vesicles are coupled processes in Bacteroides. mSphere **3**, https://doi.org/10.1128/mSphere.00559-18 (2018).
43. Li, R., and Liu, Q. Engineered bacterial outer membrane vesicles as multifunctional delivery platforms. *Front. Mater.* **7**, https://doi.org/10.3389/fmats.2020.00202 (2020).
44. Zingl, F. G., Leitner, D. R., Thapa, H. B. & Schild, S. Outer membrane vesicles as versatile tools for therapeutic approaches. *Microlife* **2**, uqab006 (2021).
45. Foley, M. H., Cockburn, D. W. & Koropatkin, N. M. The Sus operon: a model system for starch uptake by the human gut Bacteroidetes. *Cell Mol. Life Sci.* **73**, 2603–2617 (2016).
46. Sartorio, M. G., Pardue, E. J., Scott, N. E. & Feldman, M. F. Human gut bacteria tailor extracellular vesicle cargo for the breakdown of diet- and host-derived glycans. *Proc. Natl Acad. Sci. USA* **120**, e2306314120 (2023).

47. Thomas, S., Holland, I. B. & Schmitt, L. The Type 1 secretion pathway - the hemolysin system and beyond. *Biochim Biophys. Acta* **1843**, 1629–1641 (2014).
48. Bhoite, S., van Gerven, N., Chapman, M. R., and Remaut, H. Curli Biogenesis: bacterial amyloid assembly by the type viii secretion pathway. *EcoSal Plus* **8**, https://doi.org/10.1128/ecosalplus.ESP-0037-2018 (2019).
49. Garmory, H. S. et al. Salmonella enterica serovar typhimurium expressing a chromosomally integrated copy of the Bacillus anthracis protective antigen gene protects mice against an anthrax spore challenge. *Infect. Immun.* **71**, 3831–3836 (2003).
50. Goosens, V. J. et al. Komagataeibacter tool kit (KTK): a modular cloning system for multigene constructs and programmed protein secretion from cellulose producing bacteria. *ACS Synth. Biol.* **10**, 3422–3434 (2021).
51. Su, L. et al. Extracellular overexpression of recombinant Thermobifida fusca cutinase by alpha-hemolysin secretion system in E. coli BL21(DE3). *Micro Cell Fact.* **11**, 8 (2012).
52. Xu, J. et al. A genomic view of the human-Bacteroides thetaiotaomicron symbiosis. *Science* **299**, 2074–2076 (2003).
53. Hussack, G. et al. Neutralization of clostridium difficile toxin a with single-domain antibodies targeting the cell receptor binding domain. *J. Biol. Chem.* **286**, 8961–8976 (2011).
54. Song, J. H. & Kim, Y. S. Recurrent clostridium difficile infection: risk factors, treatment, and prevention. *Gut Liver* **13**, 16–24 (2019).
55. Chen, Z. Y. et al. Construction of leaky strains and extracellular production of exogenous proteins in recombinant Escherichia coli. *Micro Biotechnol.* **7**, 360–370 (2014).
56. Wurm, D. J., Slouka, C., Bosilj, T., Herwig, C. & Spadiut, O. How to trigger periplasmic release in recombinant Escherichia coli: A comparative analysis. *Eng. Life Sci.* **17**, 215–222 (2017).
57. Alav, I. et al. Structure, Assembly, and function of tripartite efflux and type 1 secretion systems in gram-negative bacteria. *Chem. Rev.* **121**, 5479–5596 (2021).
58. Khambhati, K., Patel, J., Saxena, V., A, P., and Jain, N. Gene regulation of biofilm-associated functional amyloids. *Pathogens* **10**. https://doi.org/10.3390/pathogens10040490 (2021).
59. Jarchau, T., Chakraborty, T., Garcia, F. & Goebel, W. Selection for transport competence of C-terminal polypeptides derived from Escherichia coli hemolysin: the shortest peptide capable of autonomous HlyB/HlyD-dependent secretion comprises the C-terminal 62 amino acids of HlyA. *Mol. Gen. Genet* **245**, 53–60 (1994).
60. Sevastsyanovich, Y. R. et al. A generalised module for the selective extracellular accumulation of recombinant proteins. *Micro Cell Fact.* **11**, 69 (2012).
61. Hersch, S. J., Lam, L. & Dong, T. G. Engineered type six secretion systems deliver active exogenous effectors and Cre recombinase. *mBio* **12**, e0111521 (2021).
62. Beirnaert, E. et al. Bivalent llama single-domain antibody fragments against tumor necrosis factor have picomolar potencies due to intramolecular interactions. *Front Immunol.* **8**, 867 (2017).
63. Gareb, B., Otten, A. T., Frijlink, H. W., Dijkstra, G., and Kosterink, J. G. W. Review: local tumor necrosis factor-α inhibition in inflammatory bowel disease. *Pharmaceutics* **12**. https://doi.org/10.3390/pharmaceutics12060539 (2020).
64. Roovers, R. C. et al. A biparatopic anti-EGFR nanobody efficiently inhibits solid tumour growth. *Int J. Cancer* **129**, 2013–2024 (2011).
65. Krasinskas, A. M. EGFR signaling in colorectal carcinoma. *Pathol. Res Int* **2011**, 932932 (2011).
66. Kelly, V. W. & Sirk, S. J. Short FcRn-Binding Peptides Enable Salvage and Transcytosis of scFv Antibody Fragments. *ACS Chem. Biol.* **17**, 404–413 (2022).
67. Iqbal, N. & Iqbal, N. Human epidermal growth factor receptor 2 (her2) in cancers: overexpression and therapeutic implications. *Mol. Biol. Int* **2014**, 852748 (2014).
68. Hall, M. P. et al. Engineered luciferase reporter from a deep sea shrimp utilizing a novel imidazopyrazinone substrate. *ACS Chem. Biol.* **7**, 1848–1857 (2012).
69. Heim, R. & Tsien, R. Y. Engineering green fluorescent protein for improved brightness, longer wavelengths and fluorescence resonance energy transfer. *Curr. Biol.* **6**, 178–182 (1996).
70. Mueller, K. E. & Fields, K. A. Application of β-lactamase reporter fusions as an indicator of effector protein secretion during infections with the obligate intracellular pathogen Chlamydia trachomatis. *PLoS One* **10**, e0135295 (2015).
71. Lenders, M. H. et al. Directionality of substrate translocation of the hemolysin A Type I secretion system. *Sci. Rep.* **5**, 12470 (2015).
72. Cheng, C. M. et al. Functional production of a soluble and secreted single-chain antibody by a bacterial secretion system. *PLoS One* **9**, e97367 (2014).
73. Byun, H., Park, J., Kim, S. C. & Ahn, J. H. A lower isoelectric point increases signal sequence-mediated secretion of recombinant proteins through a bacterial ABC transporter. *J. Biol. Chem.* **292**, 19782–19791 (2017).
74. Schulze-Osthoff, K. et al. Cytotoxic activity of tumor necrosis factor is mediated by early damage of mitochondrial functions. Evidence for the involvement of mitochondrial radical generation. *J. Biol. Chem.* **267**, 5317–5323 (1992).
75. Muyldermans, S. Nanobodies: natural single-domain antibodies. *Annu Rev. Biochem* **82**, 775–797 (2013).
76. Freudl, R. Signal peptides for recombinant protein secretion in bacterial expression systems. *Micro Cell Fact.* **17**, 52 (2018).
77. González-Montalbán, N., Carrió, M. M., Cuatrecasas, S., Arís, A. & Villaverde, A. Bacterial inclusion bodies are cytotoxic in vivo in absence of functional chaperones DnaK or GroEL. *J. Biotechnol.* **118**, 406–412 (2005).
78. Chen, Y. J. et al. Characterization of 582 natural and synthetic terminators and quantification of their design constraints. *Nat. Methods* **10**, 659–664 (2013).
79. Kulp, A. & Kuehn, M. J. Biological functions and biogenesis of secreted bacterial outer membrane vesicles. *Annu Rev. Microbiol* **64**, 163–184 (2010).
80. Fiocca, R. et al. Release of Helicobacter pylori vacuolating cytotoxin by both a specific secretion pathway and budding of outer membrane vesicles. Uptake of released toxin and vesicles by gastric epithelium. *J. Pathol.* **188**, 220–226 (1999).
81. Balsalobre, C. et al. Release of the type I secreted alpha-haemolysin via outer membrane vesicles from Escherichia coli. *Mol. Microbiol* **59**, 99–112 (2006).
82. Bonnington, K. E. & Kuehn, M. J. Protein selection and export via outer membrane vesicles. *Biochim Biophys. Acta* **1843**, 1612–1619 (2014).
83. Cole, G. B., Bateman, T. J. & Moraes, T. F. The surface lipoproteins of gram-negative bacteria: Protectors and foragers in harsh environments. *J. Biol. Chem.* **296**, 100147 (2021).
84. Prezza, G. et al. Comparative genomics provides structural and functional insights into Bacteroides RNA biology. *Mol. Microbiol* **117**, 67–85 (2022).
85. Coyne, M. J., Roelofs, K. G. & Comstock, L. E. Type VI secretion systems of human gut Bacteroidales segregate into three genetic architectures, two of which are contained on mobile genetic elements. *BMC Genomics* **17**, 58 (2016).
86. Sepahdar, Z., Miroliaei, M., Bouzari, S., Khalaj, V. & Salimi, M. Surface engineering of escherichia coli-derived OMVs as promising nano-carriers to target EGFR-overexpressing breast cancer cells. *Front Pharm.* **12**, 719289 (2021).

87. Gujrati, V. et al. Bioengineered bacterial outer membrane vesicles as cell-specific drug-delivery vehicles for cancer therapy. *ACS Nano* **8**, 1525–1537 (2014).
88. Alaniz, R. C., Deatherage, B. L., Lara, J. C. & Cookson, B. T. Membrane vesicles are immunogenic facsimiles of Salmonella typhimurium that potently activate dendritic cells, prime B and T cell responses, and stimulate protective immunity in vivo. *J. Immunol.* **179**, 7692–7701 (2007).
89. Wo, J. et al. Engineering probiotic-derived outer membrane vesicles as functional vaccine carriers to enhance immunity against SARS-CoV-2. *iScience* **26**, 105772 (2023).
90. Michel, L. V. et al. Dual Orientation of the Outer Membrane Lipoprotein P6 of Nontypeable *Haemophilus influenzae*. *J. Bacteriol.* **195**, 3252–3259 (2013).
91. Michel, L. V. et al. Dual orientation of the outer membrane lipoprotein Pal in Escherichia coli. *Microbiol. (Read.)* **161**, 1251–1259 (2015).
92. Dean, S. N., et al. Different strategies affect enzyme packaging into bacterial outer membrane vesicles. *Bioengineering (Basel)* **10**, https://doi.org/10.3390/bioengineering10050583 (2023).
93. Engelhart, M. J. et al. The NQR complex regulates the immunomodulatory function of bacteroides thetaiotaomicron. *J. Immunol.* **211**, 767–781 (2023).
94. Evan, J. et al. Dual membrane-spanning anti-sigma factors regulate vesiculation in *Bacteroides thetaiotaomicron*. *Proc. Natl. Acad. Sci. USA* **121**, e2321910121 (2024).
95. Chang, H. J. et al. A modular receptor platform to expand the sensing repertoire of bacteria. *ACS Synth. Biol.* **7**, 166–175 (2018).
96. Koch, M., Pandi, A., Borkowski, O., Batista, A. C. & Faulon, J. L. Custom-made transcriptional biosensors for metabolic engineering. *Curr. Opin. Biotechnol.* **59**, 78–84 (2019).
97. Lahav-Mankovski, N. et al. Decorating bacteria with self-assembled synthetic receptors. *Nat. Commun.* **11**, 1299 (2020).
98. Wexler, A. G. & Goodman, A. L. An insider's perspective: Bacteroides as a window into the microbiome. *Nat. Microbiol* **2**, 17026 (2017).
99. Guiney, D. G., Hasegawa, P. & Davis, C. E. Plasmid transfer from Escherichia coli to Bacteroides fragilis: differential expression of antibiotic resistance phenotypes. *Proc. Natl Acad. Sci. USA* **81**, 7203–7206 (1984).
100. Wilson, M. M., Anderson, D. E. & Bernstein, H. D. Analysis of the outer membrane proteome and secretome of Bacteroides fragilis reveals a multiplicity of secretion mechanisms. *PLoS One* **10**, e0117732 (2015).
101. Baneyx, F. & Mujacic, M. Recombinant protein folding and misfolding in Escherichia coli. *Nat. Biotechnol.* **22**, 1399–1408 (2004).
102. Josefsdottir, K. S., Baldridge, M. T., Kadmon, C. S. & King, K. Y. Antibiotics impair murine hematopoiesis by depleting the intestinal microbiota. *Blood* **129**, 729–739 (2017).

Acknowledgements

This work was funded by the NIH/NIBIB (1R21EB032548 to S.J.S.). We thank S. Lyu for computational identification of lead peptide sequences.

Author contributions

Conceptualization: Y.H.Y. and S.J.S.; Methodology: Y.H.Y.; Formal Analysis: Y.H.Y.; Investigation: Y.H.Y. and V.W.K.; Resources: Y.H.Y., V.W.K. and R.R.P.; Writing – Original Draft: Y.H.Y. and S.J.S.; Writing—Review & Editing: Y.H.Y. and S.J.S.; Validation: Y.H.Y.; Visualization: Y.H.Y.; Supervision: Y.H.Y.; Project Administration: S.J.S.; Funding Acquisition: S.J.S.

Competing interests

Y.H.Y. and S.J.S. have filed a patent application on the molecular toolkit developed in this study for heterologous protein secretion across *Bacteroides* species (PCT/US2023/083131). Other authors claim no competing interests.

Additional information

Supplementary information The online version contains supplementary material available at https://doi.org/10.1038/s41467-024-53845-7.

Correspondence and requests for materials should be addressed to Shannon J. Sirk.

Peer review information *Nature Communications* thanks Cammie Lesser and the other, anonymous, reviewer(s) for their contribution to the peer review of this work. A peer review file is available.